

Iyuku raathi, a new iguanodontian dinosaur from the Early Cretaceous Kirkwood Formation, South Africa

Catherine A. Forster¹  | William J. de Klerk^{2,3} | Karen E. Poole⁴  |
 Anusuya Chinsamy-Turan^{5,6}  | Eric M. Roberts⁷ | Callum F. Ross⁸

¹Department of Biological Sciences, The George Washington University, Washington, District of Columbia, USA

²Department of Geology, Rhodes University, Makhanda, South Africa

³Department of Earth Sciences, Albany Museum, Makhanda, South Africa

⁴Department of Basic Sciences, New York Institute of Technology College of Osteopathic Medicine at Arkansas State University, Jonesboro, Arkansas, USA

⁵Zoology Department, University of Cape Town, Cape Town, South Africa

⁶Earth Sciences Division, South African Museum, Cape Town, South Africa

⁷School of Earth and Environmental Sciences, James Cook University, Townsville, Queensland, Australia

⁸Department of Organismal Biology, University of Chicago, Chicago, Illinois, USA

Correspondence

Catherine A. Forster, Department of Biological Sciences, 2029 G St. NW, The George Washington, University, Washington, DC 20052, USA.

Email: forster@gwu.edu

Funding information

George Washington University; The Dinosaur Society; The Jurassic Foundation

Abstract

We name and describe a new iguanodontian dinosaur from the Early Cretaceous Kirkwood Formation, Eastern Cape Province, South Africa. This dinosaur is one of only two ornithopod dinosaurs known from the Cretaceous of southern Africa, and is unique in being represented primarily by hatchling to young juvenile individuals as demonstrated by bone histological analysis. All of the juvenile material of this new taxon comes from a single, laterally-restricted bonebed and specimens were primarily recovered as partial to complete single elements, although rare articulated materials and one partial skeleton were found. Sedimentology of the bonebed suggests that this horizon heralds a change in environment upsection to a drier and more seasonal climate. This accumulation of bones is interpreted as seasonal mortality from a nesting site or nesting grounds and may be linked to this environmental shift.

KEY WORDS

dinosaur, Early Cretaceous, Iguanodontian, morphology, ornithopod, South Africa

Abbreviations: AM, Albany Museum, Makhanda (Grahamstown), SA; IRSNB, Institut Royal des Sciences Naturelles de Belgique, Brussels, Belgium; MB.R, Museum für Naturkunde, Berlin, Germany; NHMUK, Natural History Museum, London, UK; ROM, Royal Ontario Museum, Toronto, Canada; SAM, South African Museum, Cape Town, SA; SMU, Shuler Museum of Paleontology, Southern Methodist University, Dallas, USA; USNM, National Museum of Natural History, Smithsonian Institution, Washington, DC, USA; ZDM, Zigong Dinosaur Museum, Dashanpu, PRC.

1 | INTRODUCTION

The presence of iguanodontian dinosaur material in the Early Cretaceous Kirkwood Formation of Eastern Cape Province, South Africa, was first reported by Rich et al. (1983), based on their discovery of a partial cervical vertebra. More recently, we confirmed the presence of a small iguanodontian in the Kirkwood Fm after collecting

numerous elements and a semi-articulated specimen (De Klerk et al., 1998; de Klerk et al., 2000; Forster et al., 1995; Forster & de Klerk, 2008). Here we name and describe the Kirkwood iguanodontian, *Iyuku raathi*, gen. et sp. nov.

Iyuku is part of a diverse Kirkwood fauna that includes the sphenodontian *Opisthias* (Rich et al., 1983), a lepidosaur (Ross et al., 1999), teleost and holosteian fishes (de Klerk et al., 1998; Rich et al., 1983), crocodilians, turtles, frog, sauropods (Broom, 1904; de Klerk et al., 1998), the stegosaur *Paranthodon* (Galton & Coombs Jr., 1981; Raven & Maidment, 2018), the ornithomimosaur *Nqwebasaurus* (Choiniere et al., 2012; de Klerk et al., 2000), and a non-tetanuran theropod (Forster et al., 2009). Despite an extremely long collecting history beginning in 1845 (Atherstone, 1857) the Kirkwood Fm has produced primarily isolated and often fragmentary fossils. However, numerous collecting forays into the Kirkwood Fm since 1994, spearheaded by WJD, have begun to produce more complete and informative dinosaur specimens such as the articulated partial skeleton of *Nqwebasaurus* (Choiniere et al., 2012; de Klerk et al., 2000).

The specimens described here were collected primarily during three field seasons (1995, 1997, and 1999) by WJD, CAF, and CFR with the help of many others (see Acknowledgements). Nearly all specimens come from a single, laterally restricted horizon, herein referred to as the Kirkwood Quarry, at the Kirkwood Lookout (“Cliffs”) locality on the Sundays River, 2.65 km south of the town of Kirkwood (Figure 1). This sequence of rocks also serves as the unit stratotype of the Kirkwood Fm. The majority of the specimens consist of complete or partial disarticulated elements from very small individuals; the exception is one semi-articulated skeleton (holotype AM

6150). Rare isolated elements of larger individuals were also recovered from the quarry. Mixed with the numerous remains of *Iyuku* in the Kirkwood Quarry were rare theropod teeth, crocodile teeth, turtle shell fragments, freshwater fish bones, and a lepidosaur braincase (Ross et al., 1999).

Ornithopod remains are extremely rare in southern Africa and only two taxa have been described and named. The best known and represented taxon is the small iguanodontian *Dysalotosaurus lettowvorbecki* from the Late Jurassic Tendaguru fauna of Tanzania, represented by beautifully preserved cranial and postcranial remains (Hübner & Rauhut, 2010; Janensch, 1955). The other iguanodontian is *Kangnasaurus coetzeei*, represented by dissociated postcranial elements and one tooth (Cooper, 1985; Haughton, 1915; Rogers, 1915). *Kangnasaurus* was collected from the base of the Kalahari succession on the Bushmanland Plateau in Namaqualand, Northern Cape Province, South Africa, in 1913 and 1914. The *Kangnasaurus* material was pulled piecemeal from a well drilling operation, approximately 34 m below the surface (Rogers, 1915), and belongs to at least three individuals. Neither Haughton (1915) nor Rogers (1915) attached an age to the *Kangnasaurus* material, feeling that “... speculation as to the exact age of the remains would be very premature” (Haughton, 1915, p. 264). In his redescription of the material, Cooper (1985) surmised an Early Cretaceous age for *Kangnasaurus* due to its hypothesized affinity to *Dysalotosaurus*, but noted that this was not supported by any geological evidence. De Wit et al. (1992) investigated the *Kangnasaurus*-bearing deposits and provided geological evidence that they represent the infilling of a crater lake formed over a kimberlite pipe intrusion, similar to that described by Smith (1986) for the Stompoor crater site, Northern Cape,

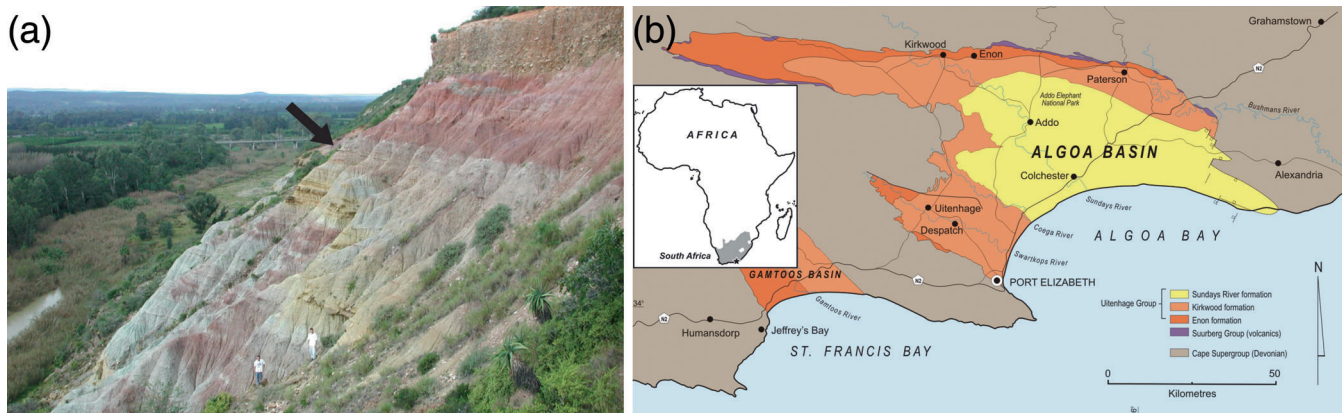


FIGURE 1 (a) Kirkwood Lookout locality, the unit stratotype of the Kirkwood Fm. The location of the *Iyuku* quarry near the top of the section is indicated by the arrow. (b) Location map showing the extent of the Uitenhage Group in the Algoa Basin. The Kirkwood Lookout locality is immediately south of the town of Kirkwood on the south side of the Sundays River

South Africa. Since intrusives in the *Kangnasaurus* area are Late Cretaceous in age (or younger), de Wit et al. (1992) suggest a Late Cretaceous age for the bone-bearing sediments.

Norman (2004) regarded *Kangnasaurus* as a *nomen dubium*, although the material certainly pertains to an iguanodontian based on morphology including the presence of a prominent central ridge on the teeth, a tall and robust lesser trochanter on the femur, a cranial intercondylar sulcus on the distal femur, a caudal intercondylar sulcus on the distal femur that is partially covered caudally by an inflated medial condyle, and a lateral condyle inset from the lateral edge of the femur. Poole (2015) considered *Kangnasaurus* to be a valid iguanodontian taxon basal to Ankylopellexia. *Iyuku* is the only known iguanodontian from the Early Cretaceous of southern Africa, and together with *Kangnasaurus* they comprise the entire Cretaceous record of ornithopods in southern Africa.

2 | SEDIMENTOLOGY AND STRATIGRAPHY OF THE KIRKWOOD FM

The Kirkwood Fm is one of three units that comprise the Uitenhage Group, a thick sequence of sedimentary fill within the Algoa Basin, the largest of several fault-controlled half-graben mid-Mesozoic sedimentary basins that lie along the southern coast of Africa (e.g., Muir et al., 2017a, 2017b; Muir et al., 2020; Tankard et al., 1982; Winter, 1973). The Uitenhage Group unconformably overlies rocks of the Paleozoic Cape Supergroup and is formally divided into the Enon Formation, Kirkwood Formation, and the Sundays River Formation (Figure 1). The Kirkwood Fm is divided into the Bethelsdorp, Colchester, and Swartkops Members and reaches 2,210 m at its maximum measured thickness (Muir et al., 2017a, 2017b). These units were deposited in the Algoa Basin, the easternmost of the numerous syn-rifting basins in the southern Cape, at the onset of the last episode of Gondwana rifting (Muir et al., 2017b, 2020).

The Kirkwood Fm consists of variegated reddish-brown, pink or green-gray silty mudstone paleosols interbedded on various scales with sandy fluvial channel fill and lacustrine facies, and interfingers with the contemporaneous conglomeratic alluvial facies of the Enon Fm (Frost, 1996; Muir et al., 2017b, 2020; Shone, 1976, 2006; Winter, 1973). The thicker units of the Kirkwood Fm are either massive or cross-bedded and wood fragments are common with paleo-currents showing a variable southerly trend. The Kirkwood Fm has a complex and disputed relationship with the estuarine and marine facies of the Sundays River Fm (McMillan, 2003; Shone, 1978;

Toerien & Hill, 1989). Whereas some workers favor an interfingering stratigraphic relationship between the upper Kirkwood and lower Sundays River formations (e.g., Rigassi & Dixon, 1972; Shone, 1978), McMillan (2003) argued for a sharp, unconformable contact, and non-synchronous deposition of the overlying Sundays River Formation. More recent studies have supported an interfingering relationship, in part, between the Kirkwood and Sundays River formations (Muir et al., 2017a). Strata of the Uitenhage Group are largely covered by a veneer of terrestrial and marine Miocene–Pliocene Alexandria Fm (mixed siliclastics and carbonates), and alluvial terrace gravels (in the Sundays River area) of the Algoa Group. The Kirkwood Lookout section is from the top of the Kirkwood Fm and is overlain by these alluvial gravels (Figure 2). Kirkwood Fm strata are usually exposed in steep-sided river cuttings, road cuts and other discontinuous outcrops along the northern, east–west trending margin of the Algoa Basin.

Muir et al. (2017b) assigned a Tithonian to Valanginian age for the entire Kirkwood Fm. Pyroclastic deposits in the Uitenhage Group, including the Kirkwood Fm, were interpreted by Muir et al. (2020) as altered primary ash fall deposits. U-Pb dates derived from zircons from these deposits suggest that the initial deposition of the Uitenhage Group began in the late Early Jurassic and persisted into the Early Cretaceous (Valanginian; Muir et al., 2020); none of their samples came from the Algoa Basin. Work by McMillan (2003) on Sundays River Fm foraminifera indicates that the base of the Sundays River Fm in the Algoa Basin is Middle Valanginian in age. This would indicate an Early Cretaceous age (early-mid Valanginian) for the Kirkwood Fm stratotype exposure and bone-bearing fossil site, and a temporally long span of deposition for the Uitenhage Group. Muir et al. (2020) hypothesize that the deposition of the Kirkwood Fm spans this entire time range.

The Kirkwood Lookout locality is regarded as the unit stratotype exposure of the Kirkwood Fm (Reddering, 2012) and is located on the southern bank of the Sundays River, almost three kilometers south of the town of Kirkwood (site 6 of Rich et al., 1983; McLachlan & McMillan, 1976). Approximately 60 m of strata are exposed here with the bone-bearing quarry site located approximately 51 m up this sequence (Figures 1a and 2).

2.1 | Sedimentology of the Kirkwood Lookout section

The sedimentology of the Kirkwood Lookout section is characterized by an interbedded succession of mudrocks, thin sheet-like sandstone bodies, and thicker tabular to



FIGURE 2 (a) The Kirkwood Lookout exposures with the *Iyuku* bonebed (“ornithopod bonebed”) location marked with an arrow. (b) Exposures with superimposed lithofacies

lenticular sandstone bodies. Twelve primary lithofacies (LFs) are recognized at the Kirkwood Lookout section (Table 1), which in various repeated combinations form five facies associations (FAs), which are interpreted in terms of depositional environments (Figure 2b). The observed facies associations include: FA1, fluvial channels; FA2, crevasse splays and crevasse channels; FA3, weakly developed paleosols; FA4, moderate- to well-developed paleosols; and FA5, perennial ponds/backswamps (Table 2).

The fluvial channel facies association (FA1) is quite variable in terms of channel morphology and size, ranging from ~3 to >10 m in thickness and anywhere from 10's to 100's of meters wide, and characterized by lithofacies Gcm, Gmm, Se, Sp, St, Sh, Sr (Table 1). A variety of different architectural elements (*sensu* Miall, 1985) are observed within FA1, including lateral accretion macroform elements, channels, channel wings, and thin gravel

bars. Roots and burrows are restricted to the upper portions of FA1, and mostly isolated, but in some cases partially articulated, vertebrate fossils are moderately abundant in the FA, including dinosaurs, crocodiles, turtles, and fishes (de Klerk et al., 1998). Carbonized plant fragments and wood are very rare in the Kirkwood Lookout section, but are more abundant in other areas of the formation, typically in more estuarine facies to the south and east which putatively interfinger with the Sundays River Fm (Muir et al., 2017a, 2017b; Shone, 1978). Grain size in FA1 ranges from fine- to very coarse-grained sandstone, with abundant pebbly sandstone, pebble draped foresets, and pebbly conglomerate lenses. Scour and fill structures are common. The presence of lateral accretion in FA1 suggests meandering-style rivers (e.g., Smith, 1987), whereas the association of multiple fluvial channels at the same stratigraphic level, separated by floodplain mudrocks, is typically characteristic of anastomosing style river

TABLE 1 Lithofacies identified in the Kirkwood formation

Lithofacies	Description
Gcm	Clast-supported conglomerate Matrix: Mostly absent; coarse sand if present <i>Clasts</i> : Typically granule to pebble-sized, up to boulder-size; poorly sorted; sub-angular to rounded; dominantly intraformational mudstone and siltstone; rare extraformational clasts; rare clast orientation; weak normal grading
Gmm	Matrix-supported conglomerate Matrix: Medium to coarse sand; typically massive, occasionally laminated <i>Clasts</i> : Typically granule to pebble-sized; up to boulder-size; poorly sorted; sub-angular to rounded; dominantly intraformational mudstone and siltstone; rare extraformational clasts; rare clast orientation; weak normal grading
Se	Crudely stratified to massive sandstone Grain size: Coarse- to very-coarse sand with pebble sized rip-up clasts Scour fills; up to 0.5 m deep
Sp	Planar cross-bedded sandstone Grain size: Medium- to very coarse grained sand, pebbles locally common Coset thickness: 0.1–1.0 m
St	Trough cross-bedded sandstone Grain size: Medium- to coarse-grained sand, sometimes with pebbles lining foresets Coset thickness: 0.1–1.6 m
Sh	Horizontally stratified sandstone Grain size: Fine- to medium-grained sand rare parting lineation
Sr	Current ripple cross-laminated sandstone, burrows common Grain size: Very fine- to medium-grained sand
Sf	Massive to slightly laminated muddy sandstones; Grain size: fine- to coarse-grained sand; burrows or rootlets common; poorly sorted; associated with Fs, Fsm, and Fl
Fl	Finely laminated sandstone, siltstone, and claystone with very small wave ripples; burrows and roots common; rare mudcracks
Fmpl	Massive to partially laminated mudstone with rare to abundant burrows/rootlets, green to orange color horizons
Fm	Massive mudstone, bioturbation, wedge-shaped peds, rare to abundant small calcium carbonate nodules; orange to red color horizons
Fc	Massive to laminated carbonaceous mudstone moderate to rare carbonized plant material

systems (Makaske, 2001; Nadon, 1994). We interpret these features, coupled with the abundance of relatively proximally derived coarse pebble lenses as evidence of relatively proximal yet low gradient channels with stable banks draining nearby highlands. Alternatively, the alternation between meandering and anastomosing channel characteristics may reflect changes in river morphology due to fluctuating sea level (Törnqvist, 1993).

The crevasse splays and crevasse channel facies association (FA2) is characterized by thin (20–60 cm) sheet-like and laminated sand architectural elements that are typified by LFs St, Sr, and Sh (Table 1). Root traces are occasionally present and dominated by vertical tubules, whereas burrows are more common and dominated by simple *Planolites*, *Skolithos*, and meniscate backfilled burrows. Isolated bones and carbonized wood are present,

but rare. In certain cases, clear crevasse splay sandstone bodies have been heavily overprinted by rhizoturbation and other soil-forming processes, and these units are placed into FA3, rather than FA2.

The weakly developed paleosol facies association (FA3) is the most abundant facies association in the lower two-thirds of the local stratigraphy. It is characterized by lithofacies Fmpl, Sf, Sh, and Sr (and less commonly Fl and Fm; Table 1) and typified by drab gray-green to pale grayish red colors. Beds range from ~0.1 to 2 m thick, with some original bedding often visible, but moderately to heavily overprinted by roots and burrows, and in some cases shrink and swell structures (pedogenic slickensides). Isolated, and in some cases associated or partially articulated, vertebrate fossils are rare, but present. This facies association is interpreted to represent a

TABLE 2 Facies associations identified in the Kirkwood formation

Facies association	Facies	Biogenic structures	Macrofossils	Architectural elements
FA1 Fluvial channel	Gcm, Gmm, Se, Sp, St Sh, Sr	Roots and burrow at top of channels	Isolated-partially articulated dinosaurs, turtles, mollusks, wood	Lateral accretion; channels; channel wings; gravel bars
FA2 Crevasse splays and crevasse channels	St, Sr, Sh	Planolites, Skolithos, burrows, root traces	Isolated bones; wood	Sheet sand; laminated sand
FA3 Weakly developed Paleosols	Fmpl, Sf, Sr, Sh; rare Fl, Fm	Root traces, burrows	Isolated-associated dinosaurs, crocodiles, turtles, fish, bivalves, gastropods, leaves, carbonized plant fragments	Overbank fines
FA4 Moderate- to well-developed paleosols	Fm, Fmpl, Sf	Root traces, burrows	Isolated-associated dinosaurs, turtle eggshell, fish, lizards	Overbank fines
FA5 Perennial ponds/backswamps	Fl, Fc	Burrows	Microsites dominated by dinosaur, crocodile, and fish teeth; crocodile scutes, carbonized plant fragments	Overbank fines

variety of floodplain settings, dominated by fine-grained mudrocks and sandstones that were subjected to short-term surface exposure and minor pedogenesis. Most FA3 units can be classified as protosols or vertic protosols (*sensu* Mack et al., 1993).

Facies Association 4 represents moderate- to well-developed paleosols, and is characterized by distinctive light red, orange, pink, reddish brown, and deep red horizons comprised of lithofacies Fm, Fmpl, and Sf (Table 1). Beds range from a 0.2 to 3.5 m thick, and are characterized by vertic features with weakly to moderately well-developed soil horizons. Moderate to intense bioturbation is present, ranging from mottling to clay-filled rhizoliths. Shrink and swell structures (pedogenic slickensides), rare clastic dikes, angular blocky to wedge-shaped peds are often present, and in some cases, carbonate deposits are also observed. Discrete carbonate nodules tend to be small and relatively uncommon in the Kirkwood Lookout section, whereas more diffuse or wispy calcitic seams are more common. Most paleosols in FA4 can be classified as either vertisols or calcic vertisols, with some calcisol (Mack et al., 1993).

Facies Association 5 represents perennial pond and backswamp deposits, dominated by facies Fl and Fc, which are exclusively green to gray green mudstones and siltstones (Table 1). These units are rare and generally quite thin, up to 1-m thick, and often preserve some primary planar laminations, moderate to intense burrowings, but no paleosol features. Vertebrate fossils are dominated by aquatic vertebrates, including fish teeth and crocodile teeth and osteoderms. Rare carbonized plant fragments also exist.

The combination of facies associations observed at the Kirkwood Lookout locality indicates a fluvial-floodplain system. A distinctive up-section shift is observed between abundant channels (FA1) and weakly developed floodplain paleosols (FA3) to fewer channels and a higher proportion of well-developed paleosols (FA4). This suggests either a general drying trend through the section, with increasing aridity leading to fewer channels and/or more intense weathering, or a shift in the loci of the main channel belts, leading to better drained soils and slower sedimentation rates in this portion of the section (Retallack, 1990). The distinctive shift in alluvial architecture and paleosol maturity, from FA3 to FA4, occurs at roughly the same level as the *Iyuku* bonebed.

2.2 | Sedimentology of the *Iyuku* bonebed

The quarry site occurs about three quarters from the top of the left-hand side of the Kirkwood Lookout exposures, within a series of interbedded pedogenically modified floodplain mudrocks (FA3 and 4) and crevasse splay sandstones (FA2; Figure 2). The fossil horizon itself lies within an upward coarsening 110-cm thick reddish brown (10R 3/4) mudstone unit (FA4) containing clay-filled rhizoliths, slickensides, wedge-shaped peds, and very minor, small CaCO₃ glaebules. This bone-bearing FA4 sequence is interpreted as a single paleosol horizon, which is overlain by a gently erosive crevasse splay deposit (FA2). The fossil horizon is located near the base

of the paleosol (Figure 3). It is composed of 60–70% clay, 30–40% silt, and 5–10% sand, and contains a higher concentration of mottling and clay glaebules than elsewhere in the unit. Clay coated cracks and tubules, and voids are common and some rhizoliths and tubules are filled with sparry calcite; rare intraclasts also occur (Figure 4). The presence of shrink-swell structures (e.g., pedogenic slickensides and wedge-shaped peds) coupled with minor mottling and clay cutans is consistent with the definition of a Vertisol (Mack et al., 1993), a type of soil that typically develop under conditions of seasonal availability of water and homogenization of the soil profile by pedoturbation. The combination of these soil forming features suggest that the bones are situated within the Bss (slickenside) horizon of this Vertisol.

3 | THE ONTOGENETIC STAGE OF *IYUKU* SPECIMENS

Forty-six complete to partial femora have been recovered from the quarry, more than any other element. This provides the most accurate count for the minimal number of individuals recovered at the quarry site, as well as an estimate of the range of sizes. Based on non-overlapping parts of left femora (the more numerous side present in the sample), at least 27 individuals are represented in the Kirkwood Quarry sample. Complete femora range in size from 18.4 to 54.7 mm total length ($n = 12$).

The vast majority of the elements of *Iyuku* recovered from the Kirkwood Quarry and elsewhere in the formation are of very small individuals (median femoral length 36.6 mm), some with notably striated surface texture and underdeveloped articular surfaces (e.g., AM 6163, femur 18.4 mm total length; Figure 5). In addition to their small

size, all skull elements are unfused and disarticulated, all neurocentral sutures in vertebrae are open (Brochu, 1996), and a notably porous and long-grained surface texture is present (e.g., Sampson et al., 1997; Tumarkin-Deratzian et al., 2006, 2009; Figure 5). Elements from larger, subadult individuals of the same taxon have been recovered from the Kirkwood Quarry and elsewhere in the Kirkwood Fm (e.g., AM 6030; see below).

To examine the ontogenetic stage of the specimens in our sample, five isolated elements were selected for histological analysis. Four of these samples span the size range of the small juvenile sample from the Kirkwood Quarry and include a distal right tibia (AM 6005), a proximal right femur (AM 6004), and two femoral shafts (AM 6168, AM 6119). Additionally, the tibial midshaft of a much larger specimen (AM 6030; midshaft diameter 34.3 mm) was also examined. AM 6030 was collected from an unknown location on the Kirkwood Lookout exposure in 1986 by Drs. Michael Raath and Gideon Rossouw. Thin sections of each bone were prepared according to the methodology outlined by Chinsamy-Turan (2005).

The smallest individual represented in the histological samples was the femoral mid-shaft of AM 6119 with an average cross-sectional diameter is about 3 mm (Figure 6). By contrast, *Maiasaura* nestlings have a femoral diameter of 10 mm (Horner et al., 2000). Based on other complete femora in the collection, AM 6119 would represent a femur of approximately 30 mm in length. In this specimen, the bone wall varies in thickness along the shaft between 220.5 and 1,630.7 μm . AM 6119 shows a highly porous, woven bone matrix in the early stages of fibrolamellar bone deposition (Figure 6a). The large open channels, occupied in life by blood vessels and lymph tissue, will later be infilled with lamellar bone deposits to form primary osteons (e.g., Chinsamy-Turan, 2005). This

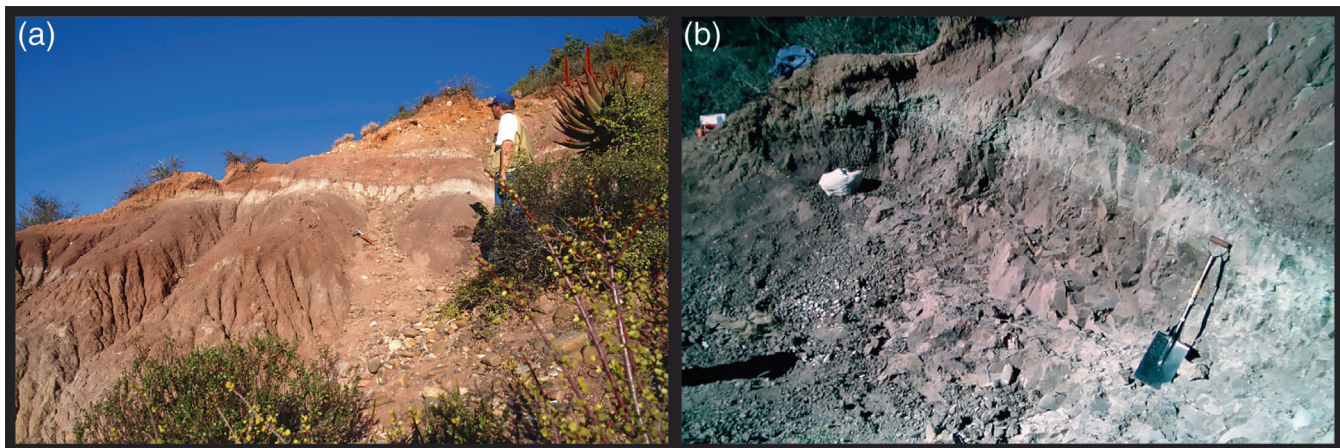


FIGURE 3 (a) The *Iyuku* quarry shortly after discovery. All elements were recovered from the lower 30 cm of the dark red mudstone. (b) The quarry after the final 1999 field season

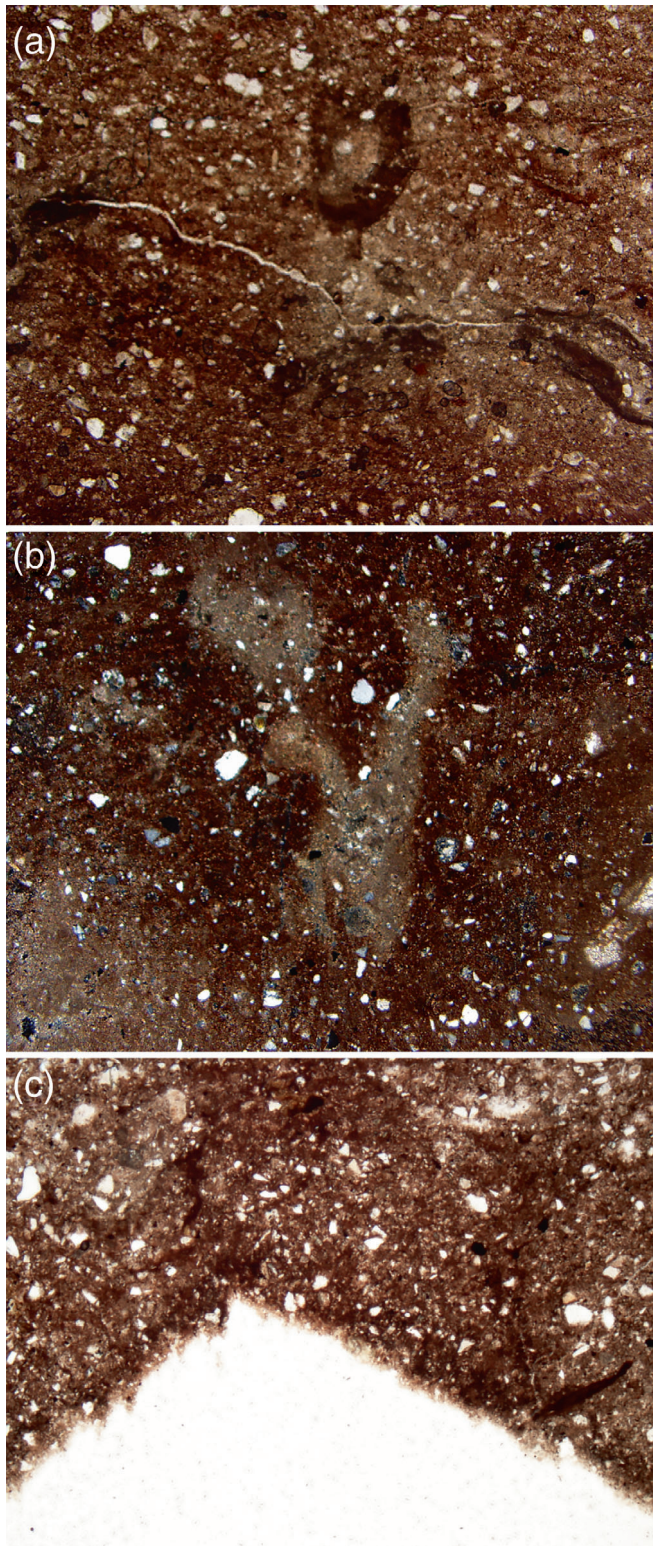


FIGURE 4 Thin section of mudstone from the quarry in plane polarized light. (a) The base of the bone-bearing level showing rare quartz sand grains, mottling, and clay globules. (b) Thirty centimeters above the base of the bone-bearing unit showing rare quartz sand grains, intense mottling, tubules with clay coatings, and sparry calcite fillings. (c) The bone-bearing layer in plane polarized light. The angular white space marks where a bone has been removed. Note the dark halo along the margin of the bone cavity



FIGURE 5 Left femur of a hatchling specimen of *Iyuku* (AM 6163) showing the striated surface texture and unfinished distal condyles

suggests that the bone is being rapidly deposited. The periosteal and endosteal margins are highly resorptive, indicating that the bone is growing in diameter and that the medullary cavity is expanding. At higher magnification (Figure 6b) radially directed struts of bone are observed in the deeper parts of the bone wall that were formed during an even earlier stage of ontogeny when an increase in girth (i.e., appositional growth) was even more rapid. In a section cut just below the fourth trochanter, the radial orientation of the channels in the direction of the trochanter shows how the bone drifts outwards to form the trochanter. These larger more radial tracts of bone are similar to that observed in embryonic dinosaurs such as *Hypacrosaurus stebingeri* (Horner & Currie, 1994), *Troodon*, and a lambeosaurine dinosaur (Horner et al., 2001). However, the outer parts of the bone wall are more similar to that of the nestling stages. This suggests that AM 6119 is a very young hatchling.

AM 6004 and AM 6005, a femur and tibia respectively, are nearly identical in their bone histology. Three thin sections were cut for AM 6004 from proximal to distal on the femoral shaft (Figure 7). As with AM 6119, radially directed struts of bone are evident from earlier episodes of rapid bone deposition, and drift outward towards the fourth trochanter (Figure 7a,b). The overall bone tissue is primarily fibrolamellar. The cross sections

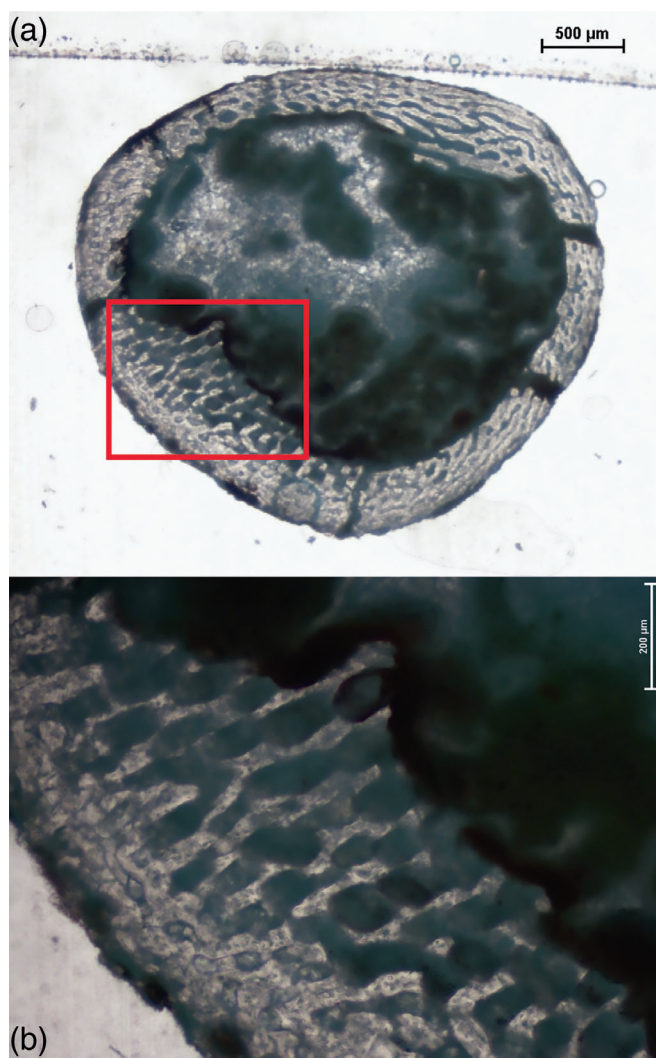


FIGURE 6 Bone histological slides through the femur of a hatchling specimen of *Iyuku*, AM 6119. (a) Slice through the entire femoral shaft, average diameter 3 mm. The red box indicates the portion of the section depicted in b. (b) Magnified view of the highly porous fibrolamellar bone. The bone wall averages 396 μm in thickness

are not symmetrical due to a large amount of resorption along the endosteal margin (Figure 7a). The medullary cavity is large and vacant towards midshaft, but is filled with cancellous bone closer to the proximal end. Three rest lines, or lines of arrested growth (LAGs) are evident: the inner two are not very distinct and cannot be traced around the compacta, whereas the peripheral rest line is quite prominent (Figure 7b). The innermost rest line does not appear to be a hatching line since the bone is already becoming compacted. In a thin section sampled from a more proximal region of the femur, evidence of reconstruction and remodeling extends nearly to the periphery of the compacta. A longitudinal section of the proximal end of the femur shows a large amount of calcified cartilage and a few struts of endochondral bone (Figure 7c).

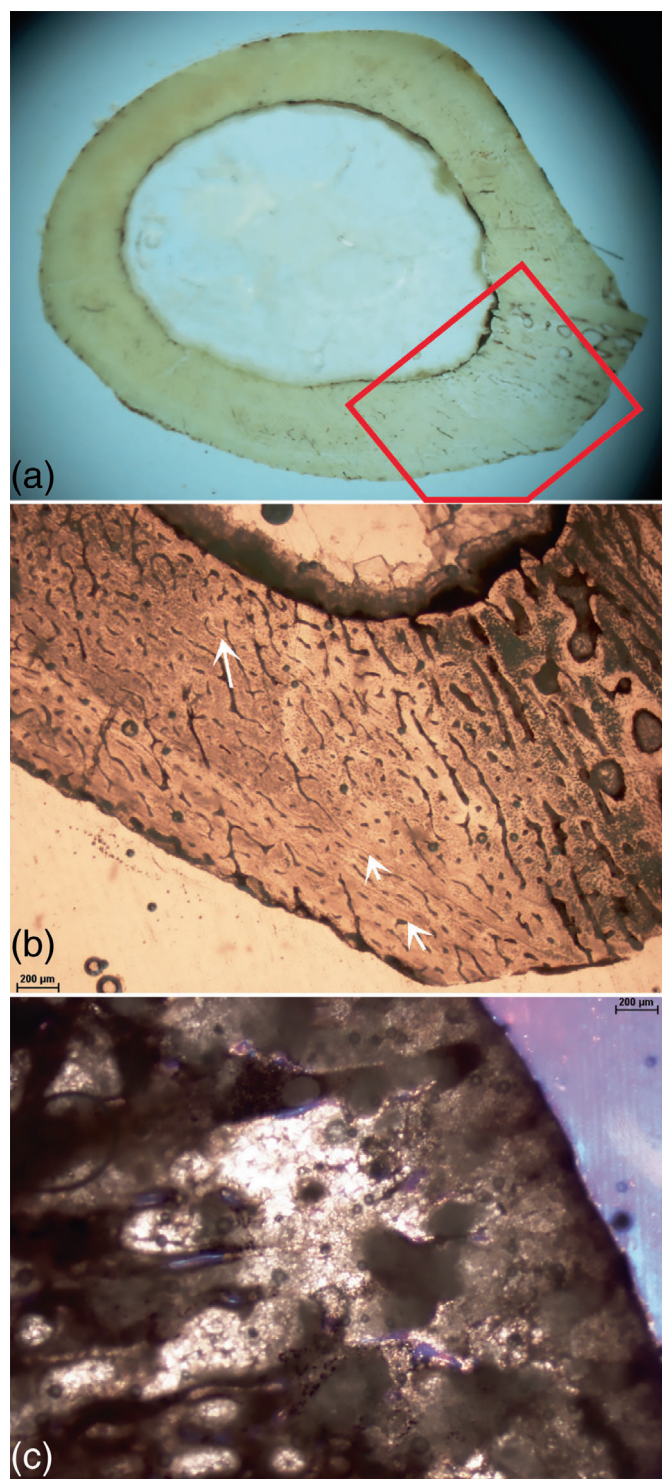


FIGURE 7 Bone histological slides through the femur of a juvenile specimen of *Iyuku*, AM 6004. (a) Slice through the entire femoral shaft just below the fourth trochanter (lower right). The red box indicates the portion of the section depicted in b. (b) Magnified view of the trochanteric region showing the fibrolamellar bone texture and the radial organization of the bone channels drifting outwards towards the trochanter. Faint growth rings are noted with arrows. (c) The articular end of the femur exhibiting a large amount of calcified cartilage and struts of endochondral bone

Extensive development of calcified cartilage at the condylar ends of the bone has been observed in young hatchlings of *Maiasaura* (Horner et al., 2000).

Thin sections of AM 6005 (tibia) show similar histology (Figure 8a,b). The bone wall is not uniform in organization or thickness and distinctive regions of secondary remodeling (such as drift) are evident (Figure 8a). Two rest lines interrupt the rapid bone deposition. Compacted, coarse cancellous bone is evident in part, and the endosteal margin is highly resorptive. In both AM 6004 and 6005, bone is beginning to become compacted but is still largely cancellous.

The thin section for AM 6168 (right femoral shaft; 7.2 mm average diameter, estimated total length 6 cm) was cut from just below the fourth trochanter (Figure 8c). The large medullary cavity at this level is empty. The bone wall is well compacted and contains a number of channels in a reticular arrangement. A single rest line may be visible close to the periphery in part but cannot be traced all the way around the circumference of the bone. The endosteal bone wall is still clearly resorptive and in places cuts into the periosteal bone tissue.

AM 6030 is a relatively large tibia lacking a portion of its shaft. Its total length, based on complete tibiae from the collection, is estimated to be at least 42 cm, or five times the length of the largest juvenile tibia from the quarry site (AM 6089, 8.4 cm long). The entire bone consists of primary tissue and is richly vascularized (Figure 9). No erosion cavities or secondary osteons are present, and bony struts are reticular in organization (Figure 9b). Rest lines are not clear in the compacta although one possibly occurs in the mid-compacta and a second near the medullary cavity, but neither is distinctive. The endosteal surface shows some signs of resorption, however no endosteally formed bone is evident, suggesting the medullary cavity is still expanding. The histology shows that this is fast growing bone without evidence of slowed deposition or of secondary reconstruction.

The bone histology can separate the sampled *Iyuku* specimens into at least four size classes: three of them representing juvenile phases of growth and the fourth depicting a larger subadult. The youngest size class appears to be a post-hatching stage and is represented by AM 6119. It has bone tissue that is reminiscent of known embryonic bones, but the outer cortex seems to have a different rate of bone deposition, suggesting that it is post-hatching. The second size class represents young juveniles (i.e., not recently hatched) and includes AM 6004 and 6005. Here the bone walls of the femur and tibia still have a large amount of open channels suggestive of rapid bone formation, although they are being compacted by the deposition of lamellar bone. The third size class, with well-compacted bone walls, is represented by AM 6168. The fourth size

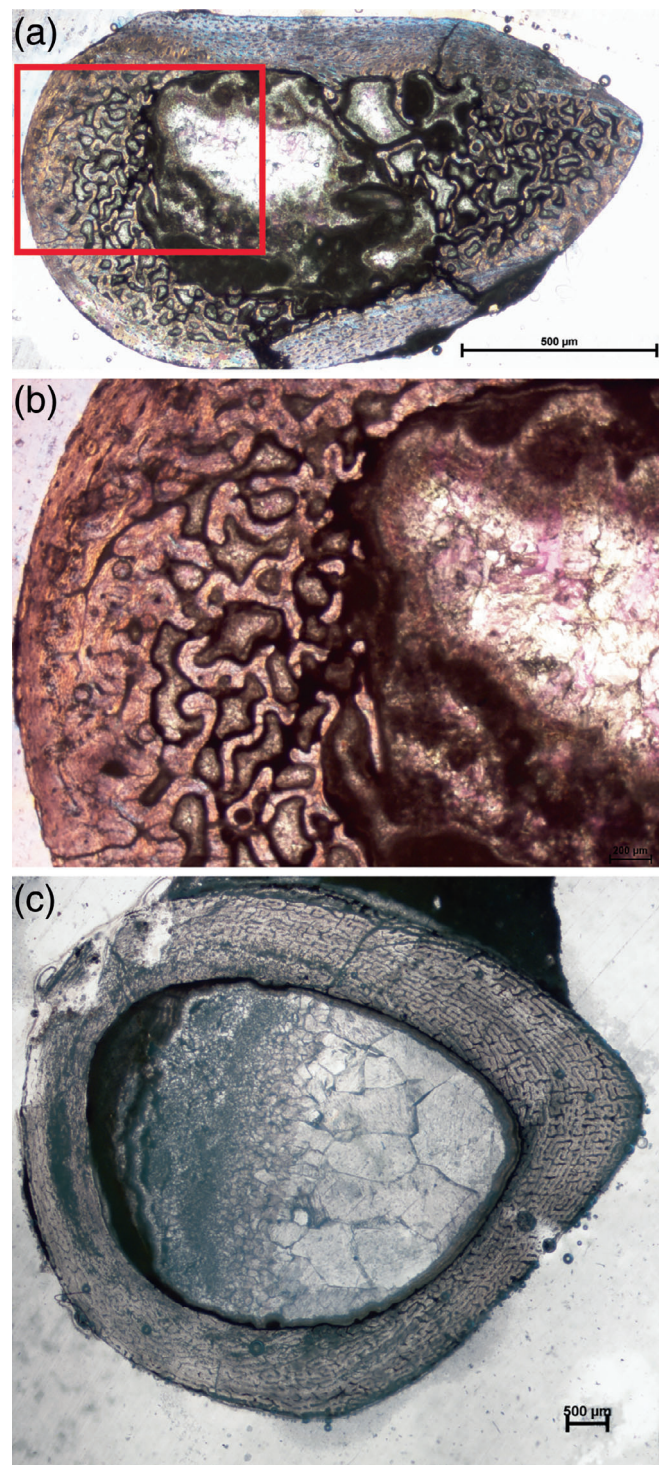


FIGURE 8 Bone histological slides through the femora of two juvenile specimens of *Iyuku*. (a) Slice through the entire femoral shaft of AM 6005 just proximal to the fourth trochanter. The bone is not uniform in organization and shows regions of secondary reconstruction. The red box indicates the portion of the section depicted in b. (b) Magnified view of AM 6005 showing the resorptive endosteal margin. (c) Section through the entire shaft of AM 6168. The bone wall is well compacted with a large, open medullary cavity

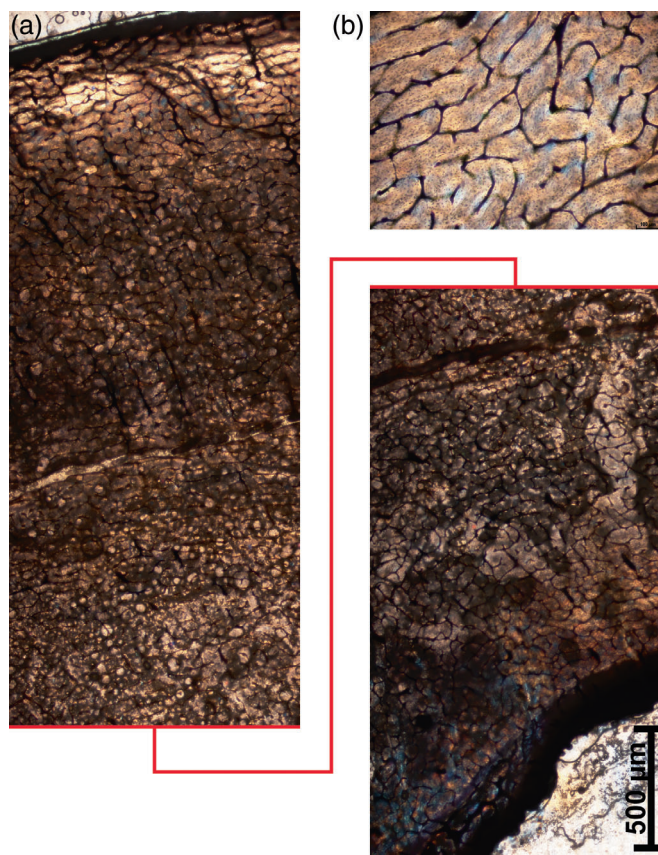


FIGURE 9 Bone histological slides through the tibia of a large juvenile specimen of *Iyuku*, AM 6030. (a) Section through the entire bone showing primary bone tissue, and an absence of either secondary osteons or erosion cavities. The long section is broken into two parts connected by the red line. (b) Magnified view from near the periphery of the bone showing its reticular organization

class, represented by AM 6030, is from a much older stage than our juvenile samples, and most likely a subadult stage since it lacks the bone microstructure typical of adults (i.e., an EFS or OCL; Chinsamy-Turan, 2005).

Unlike the situation in larger *Maiasaura* juveniles (Horner et al., 2001) juveniles of *Iyuku* lack any evidence of secondary osteons, even in the larger, sub-adult specimen (AM 6030). Another unusual feature is that faint rest lines are seen more easily in the young juveniles than in the larger individual. It may be that growth (and bone deposition) in the younger individuals is more affected by changes in environmental conditions (see below). In contrast, the femur of a juvenile *Lesothosaurus* (13 mm diameter) shows essentially fibrolamellar bone in the cortex without any secondary construction and no rest lines (Knoll et al., 2010).

Indistinct rest lines have been reported in other ornithopods, including *Dysalotosaurus* (Hübner, 2012) and *Gasparinisaura* (Cerda & Chinsamy, 2012). Cerda and Chinsamy (2012) suggested that ornithopods have more plasticity in terms of their response to environmental conditions, which may explain the variability in

occurrence of rest lines. Plasticity in response to prevailing environmental conditions has also been demonstrated in the polar hadrosaur *Edmontosaurus* (Chinsamy et al., 2012). Because of their early ontogenetic stage of these *Iyuku* specimens, it is reasonable to conclude that the multiple, faint rest lines do not represent annual growth lines. However, factors other than seasonal variability can result in temporarily slowing or stopping growth. We hypothesize that these interruptions in growth in *Iyuku* individuals are indicative of repeated stress, possibly environmentally induced, that was strong enough to cause a temporary arrest in bone deposition during their early stages of ontogeny (see taphonomy section below).

4 | TAPHONOMY OF THE *IYUKU* BONEBED

Many disarticulated, and in rare cases articulated, bones were quarried from a 20–30 cm. thick horizon exposed on a steep sided outcrop over a lateral distance of 6 m and a maximum extent into the hillside of 2.5 m (~15 m² of excavated surface; Figure 3). The bones were matrix-supported and often surrounded by narrow, pale green-gray reduction halos (Figure 4c). Bones were scattered throughout the horizon with no apparent preferred orientation of long bones and only five instances of articulation: the holotype (AM 6150; see below), AM 6015 (a distal left tibia, proximal left fibula, astragalus, and two partial metatarsals), AM 6053 (articulated left maxilla and dentary), AM 6122 (portion of a skull), and AM 6066 (cervical vertebrae and preceding two neural arches). Both complete and fragmentary elements were recovered.

The seemingly random scatter of mostly-isolated elements of varying sized hatchling to juvenile individuals mimics that reported by Horner (1994) for juvenile remains of the ornithopods *Orodromeus*, *Maiasaura*, and *Hypacrosaurus*. In these cases, disarticulated juvenile elements were scattered over surfaces interpreted as nesting grounds; eggshell and nests were largely restricted to limited portions of these nesting grounds although some eggshell fragments were occasionally found among the bones. Horner (1994) interpreted these scatters of juvenile elements, covering a range of sizes, as representing a seasonal aggradation of juvenile mortality near a nesting site.

A similar interpretation may explain the concentration of juvenile materials recovered from the Kirkwood Quarry. No dinosaur eggshell was recognized or excavated from the quarry site during the collection of the specimens, or from elsewhere in the Kirkwood



FIGURE 10 Femur of *Iyuku* in place in the quarry demonstrating the vertical orientation of some of the elements

Fm. Given the restricted size of the Kirkwood Quarry excavation, the absence of nests or eggshell is perhaps not surprising. If the Kirkwood Quarry specimens represent seasonal attrition at or near a nesting site, the random scatter of mostly disarticulated elements in the paleosol may be due to trampling prior to burial and/or bioturbation shortly after interment. The unstable, self-mulching nature of vertisols may have also contributed to post-burial movement and randomization of elements within the Bss horizon. The surface of a vertisol, due to the shrink–swell properties of their clays, desiccates into a blocky, mosaic pattern of cracks and voids reminiscent of deep mudcracks. Bones scattered across the surface could have fallen into these voids and been subsequently buried. The vertical and near-vertical orientation of some of the bones is consistent with this hypothesis (Figure 10).

5 | PHYLOGENETIC PLACEMENT OF *IYUKU*

Iyuku was included in a phylogenetic analysis of Iguanodontia by Poole (2015). A major problem in placing *Iyuku* into a phylogenetic analysis is the early ontogenetic stage of most of the material. For example, maxillae and dentaries are known only for small juveniles where the teeth are relatively enormous and tooth counts are far below

those of adults. Where a character was known to be ontogenetically variable among iguanodontians, Poole coded these characters as missing for *Iyuku*. Poole's phylogenetic analysis, which included 73 taxa and 323 characters, found *Iyuku* (2015, “Kirkwood taxon”) nested well within Iguanodontia as a member of a small Dryosauridae clade (which also included *Dryosaurus* and *Dysalotosaurus*) using both parsimony and Bayesian methods. In parsimony analysis *Dysalotosaurus* and *Iyuku* optimized as sister taxa. In the Bayesian analysis *Iyuku* is the sister to *Valdosaurus*, and these taxa are sister to *Dysalotosaurus*. This is perhaps not surprising since *Dysalotosaurus* is from the Late Jurassic (Kimmeridgian) Tendaguru Fm, Tanzania, which is both temporally and geographically proximal to the Kirkwood Fm. Dryosauridae was found to be the sister group to Ankylopelta in all analyses.

6 | SYSTEMATIC PALEONTOLOGY

Dinosauria Owen, 1842

Ornithischia Seely, 1888

Ornithopoda Marsh, 1881

Iguanodontia Baur, 1891

Iyuku raathi gen. et sp. nov.

6.1 | Etymology

Iyuku (pronounced eye-yoo-koo), Xhosa for “hatchling,” in reference to the immature status of the specimens; the species honors Dr. Michael Raath for his substantial contributions to the paleontology of southern Africa, including crucial early paleontological work in the Kirkwood Fm.

6.2 | Locality and horizon

Early Cretaceous (Valanginian) Kirkwood Formation, uppermost member, paleosol facies. All specimens are from the Kirkwood Lookout locality on the Sundays River, 2.65 km. south of Kirkwood, Eastern Cape Province, South Africa. GPS co-ordinates are available to qualified researchers upon request.

6.3 | Holotype

AM 6150, a partial, semi-articulated skeleton that preserves part of the skull, vertebral centra and arches, scapulae, pelvic girdle, both hind limbs, and ribs (Figure 11).

6.4 | Referred material

AM 6004, femur; 6005, femur; 6008, femur; 6009, femur; 6010, femur; 6012, tibia; 6013, femur; 6014, tibia; 6015, tibia, fibula, astragalus, metatarsals; 6016, tibia; 6017, tibia; 6018, tibia; 6019, femur; 6020, exoccipital; 6021, maxilla; 6022, maxilla; 6026, dorsal vertebral neural arch; 6027, dorsal rib; 6028, dorsal rib; 6029, dorsal rib; 6030, tibia; 6031, dorsal vertebral centrum; 6032, pubis; 6033, pedal ungual; 6034, sacral centrum; 6035, dorsal rib; 6046, ulna; 6052, dentary and splenial; 6053, maxilla, dentary, splenial; 6054, humerus; 6056, maxilla; 6060, femur; 6063, scapula; 6065, astragalus; 6066, cervical vertebrae; 6067, sternal plate; 6070, caudal vertebrae; 6077, frontal, postorbital, exoccipital; 6088, caudal vertebrae; 6089, tibia; 6090, tibia; 6093, premaxilla; 6094, humerus; 6095, humerus; 6096, humerus; 6097, humerus; 6098, ischium; 6099, ischium; 6100, fibula; 6101, ulna; 6102, scapula; 6103, postorbital; 6104, frontal; 6107, quadrate; 6108, quadrate; 6109, surangular, angular; 6110, surangular; 6111, dentary; 6118, quadrate; 6119, femur; 6120, dentary; 6121, metatarsal; 6122, maxilla, frontal, postorbital; 6153, dentary; 6154, maxilla; 6155, dentary; 6163, femur; 6172, radius; 6173, humerus; 6174, metatarsal; 6175, scapula; 6176, scapula; 6186, sacral centrum; 6187, cervical vertebra; 6189, fibula; 6190.

6.5 | Diagnosis

Iyuku shares with other dryosaurids a centered primary ridge on the maxillary teeth, long transverse processes on



FIGURE 11 The holotype specimen of *Iyuku raathi*, AM 6150. The right scapula has been removed from the block (from the space in the lower center of the block) but all other elements are in their original position. Skull and forelimb elements are on the left and upper middle of the block, except for the postorbital located in the far lower right next to some ribs. Pelvic and hindlimb elements extend from the upper middle to the upper right of the block. Vertebral centra and ribs are scattered throughout the block

the caudal dorsal vertebrae, and a weakly developed acromion process. *Iyuku* is distinguished from other dryosaurids by maxillary crowns that are narrower than the dentary crowns, a very long postacetabular process, sternal plates with a caudolateral process, a wide and rounded scapular spine, a narrower brevis shelf, and a prepubis that lacks a ridge on the medial side.

7 | DESCRIPTION

7.1 | Skull

One poorly preserved and partial skull (AM 6077; left frontal, left postorbital, left exoccipital) is known for *Iyuku*. Most other cranial elements occur as isolated bones, although some associated materials have been recovered (e.g., AM 6150, 6053). Not all skull elements are represented: the nasal, lacrimal, quadratojugal, palatine, vomer, pterygoid, squamosal, neurocranium, predentary, articular, and prearticular and are not known. Some of the known elements are only partially preserved.

7.2 | Premaxilla

One isolated, poorly preserved left premaxilla (AM 6093) has been recovered (Figure 12). The medial, lateral, and rostral margins of the premaxilla are worn and incomplete. Most of the maxillary process is missing, and the nature of its contact with the nasal, maxilla, and other elements cannot be ascertained (but see maxilla description below). The nasal process of the premaxilla is missing its distal tip and its rostral surface is worn, obscuring the nature of its contact with the nasal and contralateral premaxilla. Despite these missing parts, the

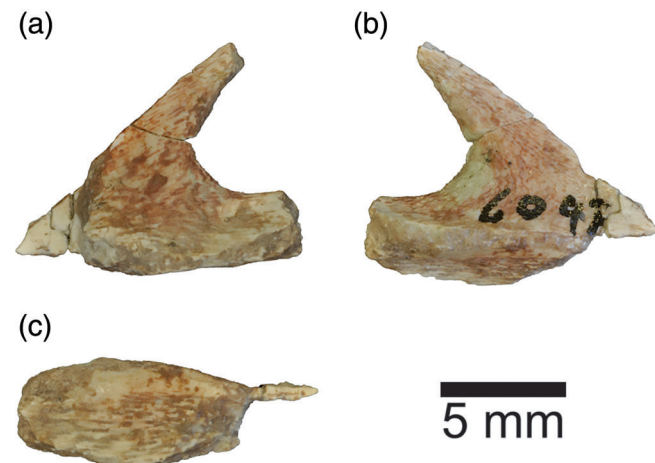


FIGURE 12 Left premaxilla of *Iyuku*, AM 6093, in (a) lateral; (b) medial; (c) ventral, rostral end to the left, views

body of the premaxilla is moderately well preserved. The premaxilla is edentulous, and the palatal portion appears to be fairly narrow and would be reconstructed to form an oval palate in ventral view (although the margins are all eroded), as in some iguanodontians (e.g., *Iguanodon*, Norman, 1980; *Equijubus*, McDonald et al., 2014; *Dysalotosaurus*, MB.R. 1322). It appears to lack the broader flare of some iguanodontians (e.g., *Ouranosaurus*, Taquet, 1976; Figure 12c). The premaxilla is smooth and rounded around the narial margin. The lateral surface of the premaxilla lacks an incised narial fossa rostroventral to the narial margin, and no foramina pierce the premaxillary body.

7.3 | Maxilla

A number of maxillae are preserved in varying states of completeness (AM 6150, 6056, 6053, 6021, 6022, 6122, 6154). The maxillary body is low and long as in other

iguanodontians (Figure 13). Three specimens preserve the mediolaterally compressed ascending process (AM 6154, medial view, Figure 13c; AM 6053; AM 6122, lateral view, Figure 13d), which is tall, acutely peaked, and rises immediately rostral to the ectopterygoid platform (Figure 13d). The ascending process is centered on the maxilla in lateral view, as in *Dryosaurus* (Galton, 1983), and its base occupies 28% the length of the maxilla in AM 6053. The free portion of the ascending process is tall, reaching 75% the height of the maxillary body at its peak. The ascending process arises near the midline of the very mediolaterally inflated maxillary body. The base of the ascending process forms the entire medial margin of the large, oval antorbital fenestra. Most of the ascending process and antorbital fenestra would have been covered laterally by the lacrimal, caudodorsal process of the premaxilla, and jugal in an articulated skull.

The maxilla is strongly emarginated above the entire tooth row (Figure 13a,d). In lateral view the dorsal

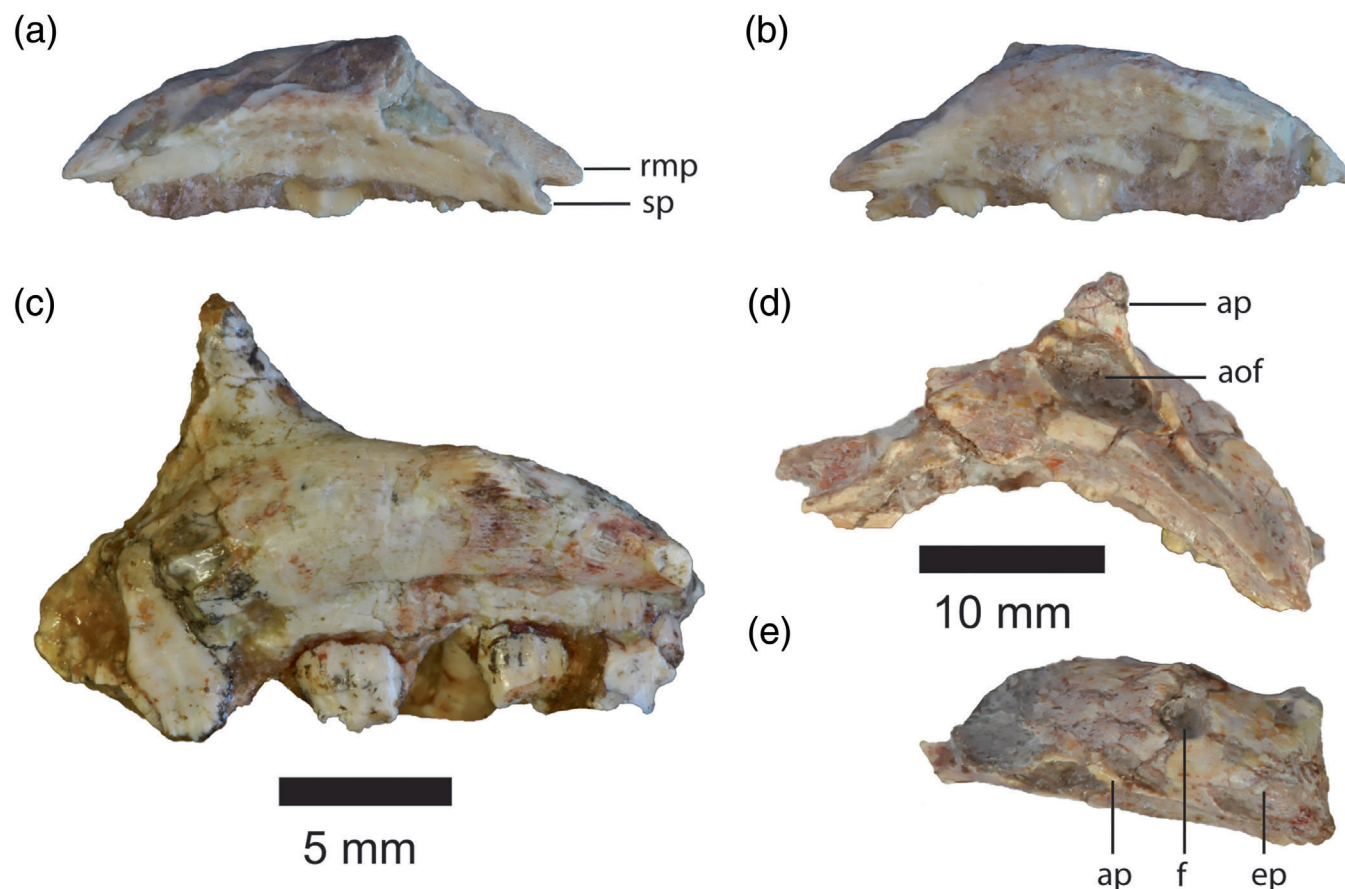


FIGURE 13 Maxillae of *Iyuku*. (a) Right maxilla of AM 6189 in lateral view. The ascending process is broken off. (b) Right maxilla of AM 6189 in medial view. (c) Right maxilla of AM 6154 in medial view showing the ascending process and a nearly complete, unworn tooth. The rostral portion of the maxilla is missing. (d) Complete left maxilla of AM 6122 (bent up dorsally) in lateral view showing the complete ascending process and antorbital fenestra. (e) Caudal portion of the left maxilla of AM 6122 in dorsal view showing ectopterygoid platform, the squared-off caudal margin of the maxilla, and the foramen just behind the ascending process. Five millimeters scale bar is for c. Ten millimeters scale bar is for all other maxillae. aof, antorbital fenestra; ap, ascending process; ep, ectopterygoid platform; rmp, rostromedial process; sp, styloid process

margin of this emargination forms a curved ridge that bows gently upward (AM 6053, 6021) and runs along the inferior margin of the antorbital fenestra. It continues caudally to the rear of the maxilla to form the dorsolateral margin of the ectopterygoid platform. A series of rostrocaudally elongate neurovascular foramina pierce the body of the maxilla on its lateral surface ventral to this ridge (Figure 13a). In ventral view the maxillary tooth row is gently curved lingually.

The rostroventral maxilla tapers to a laterally-placed styloid process that has a shallow facet on its lateral surface, presumably to fit into a socket at the rear of the premaxilla as in many ornithopods (e.g., *Zalmoxes*, Weishampel et al., 2003; Figure 13a). A single styloid process is also found in lambeosaurine hadrosaurids (e.g., *Lambeosaurus*, *Corythosaurus*) where it forms a platform that is overlapped dorsally by the premaxilla rather than fitting into a socket in the rear of the premaxilla. Also extending forward from the maxilla is a rostromedial process that is longer and more dorsally placed than the styloid process (AM 6056, AM 6053, AM 6122; Figure 13a,d) as occurs in many iguanodontians (e.g., *Iguanodon*, Norman, 1980; *Dryosaurus*, Galton, 1983; hadrosaurine hadrosaurs). In some iguanodontians (e.g., *Protohadros*, Head, 1998) the styloid process exceeds the rostromedial process in length.

A broad but shallow sulcus extends up the rostral-dorsal surface of the maxilla between the styloid process and rostromedial process, narrowing caudally until it terminates at the antorbital fenestra. The dorsal edge of the rostromedial process extends caudally as a low ridge that forms the medialmost dorsal margin of the maxilla and is confluent with the rostral margin of the ascending process (AM 6053). The medial surface of the rostromedial process is marked by two to three deep striations oriented rostrocaudally at the level of the diastema and the first maxillary tooth (Figure 13b). These striations likely received the rostral vomer on the palate. There is a short diastema at the front of the maxillary toothrow equal to one tooth position or less.

Caudal to the antorbital fenestra the dorsal margin of the maxilla curves downward to more closely approach the tooth row. In dorsal view this portion of the maxilla flares mediolaterally to form a broad platform for articulation with the ectopterygoid (Figure 13e). The ectopterygoid platform is arched gently from side to side and from front to back. A socket-like facet for the jugal is indented into the dorsolateral surface of the caudolateral maxilla, beginning just rostral to the caudal margin of the antorbital fenestra (Figure 13d). The jugal facet occupies approximately two-thirds of the lateral margin of the ectopterygoid platform, excluding the ectopterygoid from most of the caudolateral margin of the maxilla.

The caudal end of the maxilla is 33% wider than it is at the center of the ascending process (AM 6021; Figure 13d). The medial margin of the ectopterygoid platform is concave in dorsal view and slightly overhangs the body of maxilla. At the rostralmost extent of the medial ectopterygoid platform is a blunt medially directed process which lies slightly behind the caudal margin of the antorbital fenestra. A large, round foramen open onto the dorsal surface of the maxilla just rostral to the ectopterygoid platform and behind the ascending process (Figure 13d). The caudal margin of the ectopterygoid platform is squared off: its caudolateral corner extends behind the caudomedial one so that the slightly concave caudal margin of the maxilla angles caudolaterally. The last alveolus occurs at the caudal margin of the ectopterygoid platform.

In ventral view, the toothrow is nearly straight. As with other juvenile ornithopods (e.g., *Maiasaura*, YPM-PU 22400) the tooth count is extremely low and the teeth appear oversized relative to the jaw (Figures 13a,c and 14). Seven teeth occur in AM 6056 (15.3 mm total length), and nine teeth are present in AM 6053 (25.9 mm total length). In AM 6053, the width of the largest tooth crown (3.2 mm) is 12% the total length of the maxilla (25.9 mm). The smallest teeth are in the front of the jaw; they increase in size toward the middle of the toothrow then reduce in size towards the rear of the jaw.

7.4 | Maxillary teeth

The maxillary teeth are not as well exposed as the dentary teeth. In mesiodistal view the tooth crowns and roots are bowed laterally. A thin, uniform coat of enamel covers the ornamented labial surface and marginal denticles. The crown narrows towards the root and appears to reach its mesiodistally widest point approximately two-thirds of the distance to its apex, contrasting with the dentary teeth where the widest point is closer to the root (Figure 14).

All teeth bear a strong central apical ridge that runs the length of the crown on the ornamental (labial) surface. The apical ridge is centered on the crown. The crown is slightly concave between the apical ridge and the mesial and distal margins. Fine denticles are distributed along the margins of the crown, although the number of denticles are difficult to ascertain due to the poor preservation or exposure of all known unworn maxillary teeth. These denticles continue as fine secondary ridges on the ornamented surface of the crown, extending a short distance before disappearing, but never approaching the base of the crown. As a result, in worn teeth there are no secondary ridges (Figure 14b). The denticles are

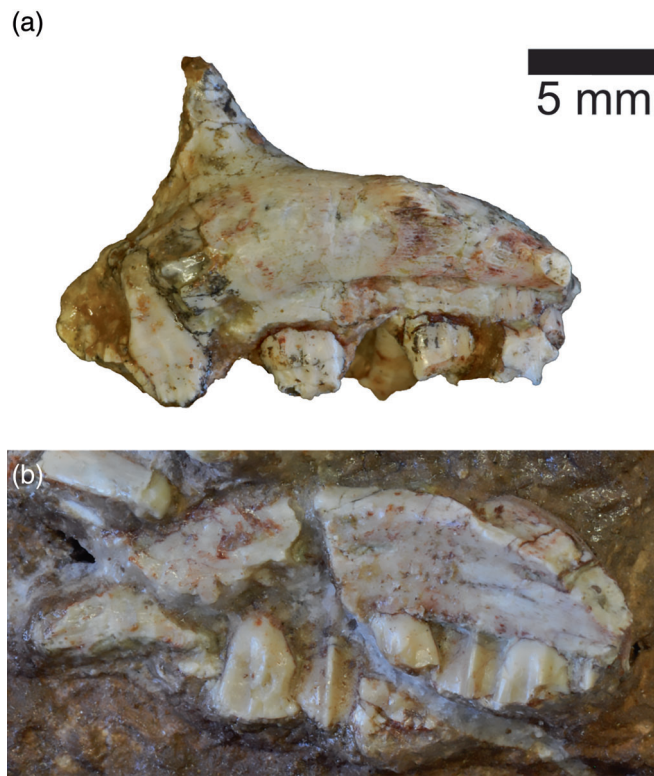


FIGURE 14 Maxillary teeth of *Iyuku*. (a) Right maxilla of AM 6150 in lateral view showing worn teeth and a partially exposed unworn tooth. (b) Right maxilla of AM 6154 in medial view showing worn and unworn teeth

slightly larger adjacent to the apical ridge, and become smaller towards the sides; the apical denticle is the largest. Wear facets are at a high angle of approximately 45° (Figure 14a).

7.5 | Frontal

At least three frontals are known: AM 6150 (left, ventral view), AM 6104 (left, dorsal view), and AM 6122 (left, dorsal, and lateral view). AM 6104 is incomplete and missing its contacts with the parietal, prefrontal, and nasals, but does preserve the postorbital contact. AM 6150 appears to be nearly complete, although its rostral margin is poorly preserved and is exposed only in ventral view, obscuring any contacts on its dorsal surface. AM 6122 is nearly complete.

The left and right frontals have an extensive midline suture with one another (Figure 15). The frontal forms the dorsal orbital margin, which is very large in *Iyuku*, not unexpected considering the early ontogenetic stage of these specimens. The orbital margin narrows laterally to a thin edge with fine parallel striations on the ventral

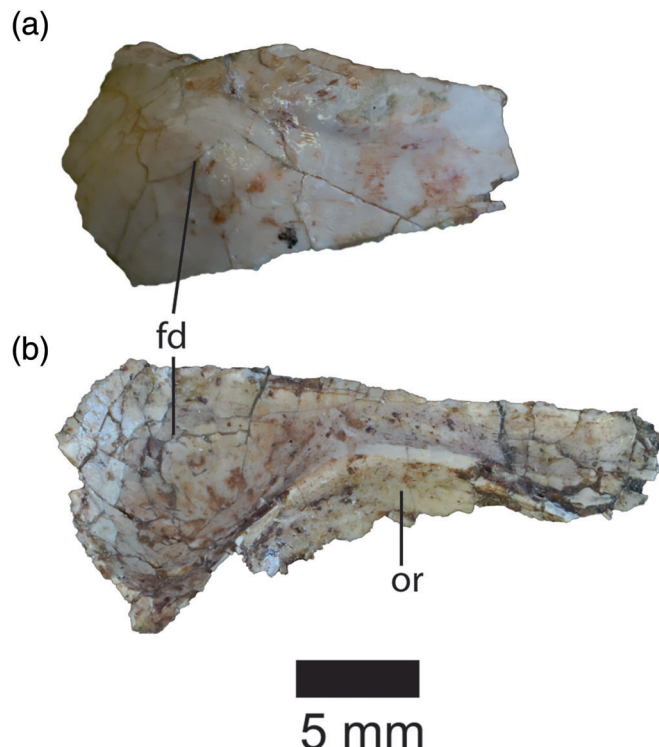


FIGURE 15 Frontals of *Iyuku*. (a) The partial left frontal of AM 6104 showing the doming of the caudal frontal, cranial end to the right. (b) The partial right frontal of holotype AM 6150 showing the interior rim and the doming of the frontal, cranial end to the right. d, dome; or, orbital rim

surface in AM 6122; no striations occur in AM 6104. There is a well-developed ventrolaterally facing “rim” on the underside of the orbital margin similar to a rim the orbital margin of the postorbital (Figure 15b).

The interorbital area is constricted and the dorsal surface of the frontals in this region is nearly flat (AM 6150). The frontal expands mediolaterally both in front of and behind the interorbital area. At the caudo-lateral margin of the frontal there is a substantial facet for the rostral postorbital. This facet is relatively broad and bears fine striations that run caudoventrally, suggesting a strong and substantial articulation between frontal and postorbital along the caudodorsal orbital margin.

Medial to the facet for the postorbital, the caudal portion of the frontal is everted into a hollow, rounded dome (AM 6150, 6104). Doming of the frontals over the rostral braincase has been noted in other juvenile ornithopods (e.g., *Gasparinisaura*, Coria & Salgado, 1996; *Lambeosaurus*, ROM 758; *Dysalotosaurus*, Hübner & Rauhut, 2010), and likely represents a juvenile feature. The contacts with the parietal, lacrimal, and nasal are not well preserved in any specimen.

7.6 | Postorbital

One partial isolated left postorbital has been recovered (AM 6103), as well as a complete right postorbital exposed in external view (AM 6150; Figure 16). The postorbital in AM 6122 is poorly preserved and preserves no margins. Along the center of the orbital margin there is a small convex palpebral process in the otherwise smooth margin (AM 6103; this area is covered by a neural arch in AM 6150; Figure 16b). Fine striations are present on the dorsal surface of the palpebral process. A similar morphology is seen in *Hexinlusaurus* (ZDM 6001) and some ornithopods (e.g., *Dryosaurus*; Galton, 1983) and likely served to anchor or support the caudal end of the palpebral.

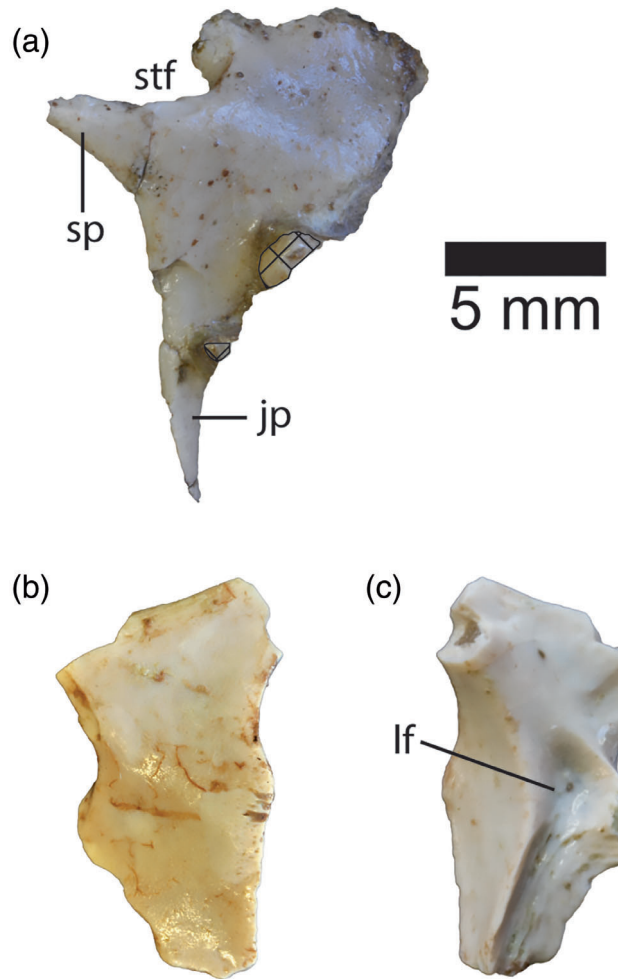


FIGURE 16 Postorbitals of *Iyuku*. (a) Right postorbital of holotype AM 6150 in lateral view showing the jugal process, squamosal process, and rostral margin of the supratemporal fenestra. Meshed areas cover underlying bone. (b) Right postorbital of AM 6103 in lateral view. (c) Right postorbital of AM 6103 in medial view showing the facet for the laterosphenoid. jp, jugal process; lf, laterosphenoid facet; sp, squamosal process; stf, supratemporal fenestra

The jugal process is long, tapers to a point, and curves gently rostrally (AM 6150; Figure 15a). The facet for the postorbital process of the jugal is not exposed; nevertheless the postorbital bar was apparently slender, as in some ornithopods (e.g., *Iguanodon*, Norman, 1980; *Hypsilophodon*, Galton, 1974). The squamosal process is short, straight, and tapers quickly to a point (AM 6150). The angle between the jugal and squamosal processes suggests that the dorsal margin of the infratemporal fenestra in *Iyuku* was quite broad.

The postorbitals preserve a short, curved section where the element contributes to the rostrolateral margin of the supratemporal fenestra (Figure 15a). A shallow, narrow, but well-defined facet for the distal postorbital process of the squamosal is present on the squamosal process of the postorbital immediately adjacent to the lateral upper temporal fenestra margin. The squamosal reached forward to nearly the rostral extent of the upper temporal fenestra. In AM 6103 the contacts between the postorbital and the frontal and parietal are mostly poorly preserved. However, the underside of the postorbital medial to the orbital rim bears a striated semi-lunar facet to allow the postorbital to broadly overlap the caudolateral frontal (Figure 16c). Immediately behind this suture is a socket-like depression that may have received the head of the laterosphenoid. The contact with the parietal is not preserved. There is a well-developed ventrolaterally facing “rim” on the medial surface of the orbital margin, similar to that under the orbital margin of the frontal (Figure 16c). From the orbital margin, the postorbital curves caudomedially then extends almost directly caudally.

7.7 | Jugal

A partial left jugal is exposed in medial view in AM 6150 (Figure 17). The right jugal is also present in this specimen although only the orbital rim is exposed (it can be seen in Figure 20a in the lower right corner). The rostral end tapers but the distal tip is broken. It is directed fully rostrally and does not curve up the rostral border of the orbit. Its dorsal margin preserves an internal rim similar to that seen on the frontal and postorbital. Its ventral margin appears straight. The articular surface for the ectopterygoid is broken although the jugal is thickened mediolaterally in that region. There is a broad facet along its rostroventral portion where the jugal overlapped the maxilla.

The tapering postorbital process extends nearly vertically from the jugal body; its distal tip is not exposed. The caudal portion of the jugal is fractured and some of the pieces are missing. However, the ventral margin of the

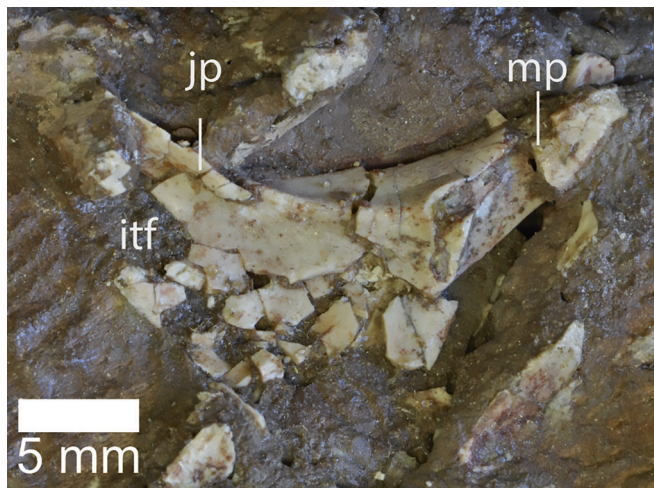


FIGURE 17 Partial left jugal of *Iyuku* (AM 6150) in medial view. The area of the ectopterygoid articulation is damaged. itf, infratemporal fenestra; jp, jugal process; mp, maxillary process

narrow lower temporal fenestra is preserved. The jugal extends a short distance up the caudoventral margin of the narrow, acute fenestra as in some ornithopods (e.g., *Dryosaurus*, Galton, 1983; *Dysalotosaurus*, Hübner & Rauhut, 2010). The distal tip of this process is also missing. Two small pieces of the caudal margin of the jugal are present and appear to show a vertical margin. However, much of the caudal margin is missing, as is the entire caudoventral margin of the jugal.

7.8 | Quadrata

A distal left (AM 6118) and two proximal quadrates (AM 6107, 6108) are preserved (Figure 18). A portion of a quadrateojugal wing is preserved in AM 6150 although it lacks both the proximal and distal ends. None of the specimens preserves the pterygoid wing.

In AM 6107, the quadrate is broken off 10 mm below the head (Figure 18a). The quadrate head is mediolaterally compressed, being wide rostrally and tapering caudally (also in AM 6108); it is nearly twice as long rostrocaudally (3.2 mm) as it is wide (1.7 mm; Figure 18c). In lateral view the rostral portion of the head is located more proximally than the caudal portion. There is a strong, short quadrate buttress (hamate process) that extends 4 mm down the caudal surface of the shaft below the quadrate head, flaring craniocaudally to 5.2 mm at its distal (widest) end. The lateral surface of the quadrate shaft is flat. Rostromedially, the base of the pterygoid wing extends in a thin plate from the lateral surface of the shaft at an angle of about 80°. The rostral surface of the proximal quadrate bears a broad vertical sulcus

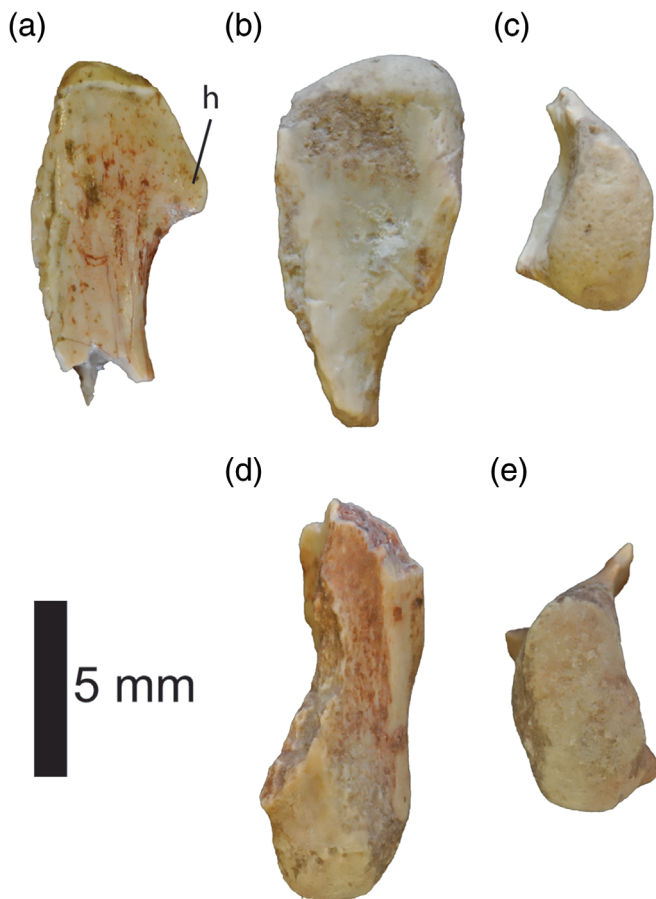


FIGURE 18 Partial quadrates of *Iyuku*. (a) Left quadrate of AM 6107 in lateral view. (b) Right quadrate of AM 6108 in medial view. (c) Right quadrate of AM 6108 in proximal view, rostral end up. (d) Left quadrate of AM 6118 in lateral view. (e) Left quadrate of AM 6118 in distal view showing the nearly equant condyles. h, hamate

separating the rostral margin of the quadrate shaft from the pterygoid wing. AM 6108 (right) preserves only 10.5 mm of the element but is in poorer condition and is identical in morphology (Figure 18b,c).

The distal quadrate condyles are poorly preserved in AM 6118 where only 11.1 mm are present (Figure 18d,e). There is no obvious division between the medial and lateral sides of a single continuous, rostrocaudally compressed condyle, similar to the situation seen in *Dysalotosaurus* (MB.R. 1320). Since the quadrate condyles are divided in all known ornithopods, the development of an intercondylar sulcus may be under ontogenetic control. In caudal view, the ventral/distal margin of the broad condyle is slightly convex. The craniocaudal length (3.3 mm) is at most 52% the mediolateral width (6.3 mm). Furthermore, the condyle narrows medially to 88% of its lateral width (3.3 vs. 2.9 mm). When the quadrate shaft is held vertically, the lateral side of the condyle projects below the medial side. This may

indicate that the quadrate shaft was directed slightly laterally in life.

The cranial surface of the distal shaft is gently concave, whereas the caudal surface very slightly convex. Although the quadratojugal wing is broken off in AM 6118, it appears to have arisen from the shaft immediately above the condyles (Figure 18d). The ventral margin of an embayment for the paraquadrate foramen is present in AM 6118, and the margin of the quadratojugal wing is abraded below this margin. A similar quadratic foramen occurs in other ornithopods (e.g., *Dryosaurus*, *Iguanodon*). In AM 6118 the base of the pterygoid flange arises immediately proximal to the condyles. Only the base of the abraded pterygoid flange is present.

7.9 | Exoccipital

The most complete portion of the neurocranium that has been identified is a partial left exoccipital (AM 6020; Figure 19). The medial portion of the exoccipital is damaged so that its contribution to the foramen magnum and

contacts with the supraoccipital and basioccipital are not preserved.

The exoccipital tapers slightly laterally, then turns sharply ventrally into a long, tapering pendant paroccipital process, as in other iguanodontians (e.g., *Iguanodon*, Norman, 1980; *Ouranosaurus*, Taquet, 1976). The preserved process in AM 6020 describes a broad arc, suggesting a sizeable gap existed between the end of the process and the braincase. The process is mediolaterally compressed with the lateral face facing slightly caudally. There is no posttemporal foramen within the paroccipital process, indicating that, if present, it occurred between the paroccipital process and the squamosal.

7.10 | Dentary

A number of dentaries are known, including both dentaries in AM 6150, a right dentary articulated with a maxilla (AM 6053), two partial left dentaries (AM 6111, 6052), a partial right dentary (AM 6120), a complete right dentary (6153), and a nearly complete left dentary (AM 6155; Figure 20). Only AM 6155 preserves a complete coronoid process (Figure 20c).

The dentary has a nearly straight ventral margin that runs parallel to the dorsal margin, and is uniform in depth along the toothrow (AM 6053, 6111, 6120, 6052; Figure 21a). In dorsal view, the toothrow is gently curved lingually. In lateral view, the toothrow is deeply inset, arising along the dorsomedial margin of the dentary, and leaving a well-demarcated buccal emargination parallel to the dorsal margin of the dentary (Figure 20b). This emargination begins at the first tooth, continues caudally, then curves upward to the rostral base of the coronoid process. A series of foramina occur along the lateral dentary just above the line of emargination.

At its rostral end the dentary curves medially, more so along the ventral aspect, and flares slightly along the ventral margin for articulation with the predentary (Figure 20b; no predentary is known for *Iyuku*). In lateral view, the upper one-third of the front of the dentary angles rostroventrally, and bears a facet along its upper margin for articulation with the dorsolateral process of the predentary. There is no diastema: the first tooth occurs immediately behind the facet for the dorsolateral process of the predentary. Below this, the rostral margin of the dentary is nearly vertical and indented by a shallow, caudoventrally oriented fossa, presumably for articulation with the caudoventral process of the predentary. A number of small foraminae occur on the rostrolateral surface of the dentary.

On the medial surface, the rostroventral dentary is also indented by a shallow fossa which may have

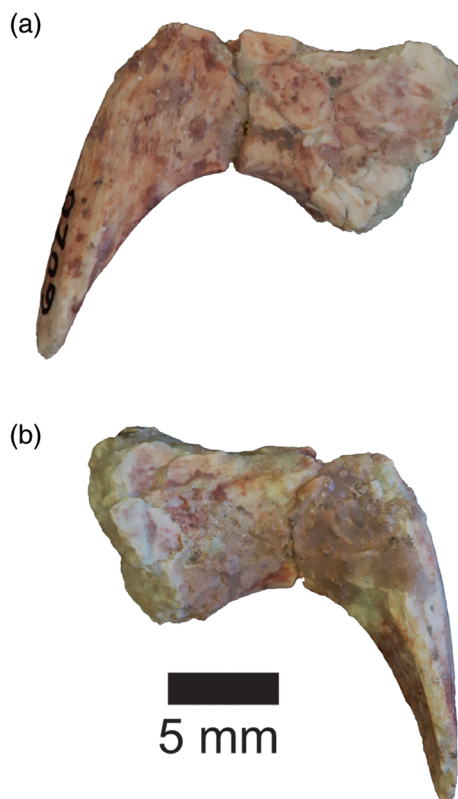


FIGURE 19 Partial left paroccipital process of *Iyuku*, AM 6020, in (a) caudal view, medial end to the right; (b) rostral view, medial end to the left

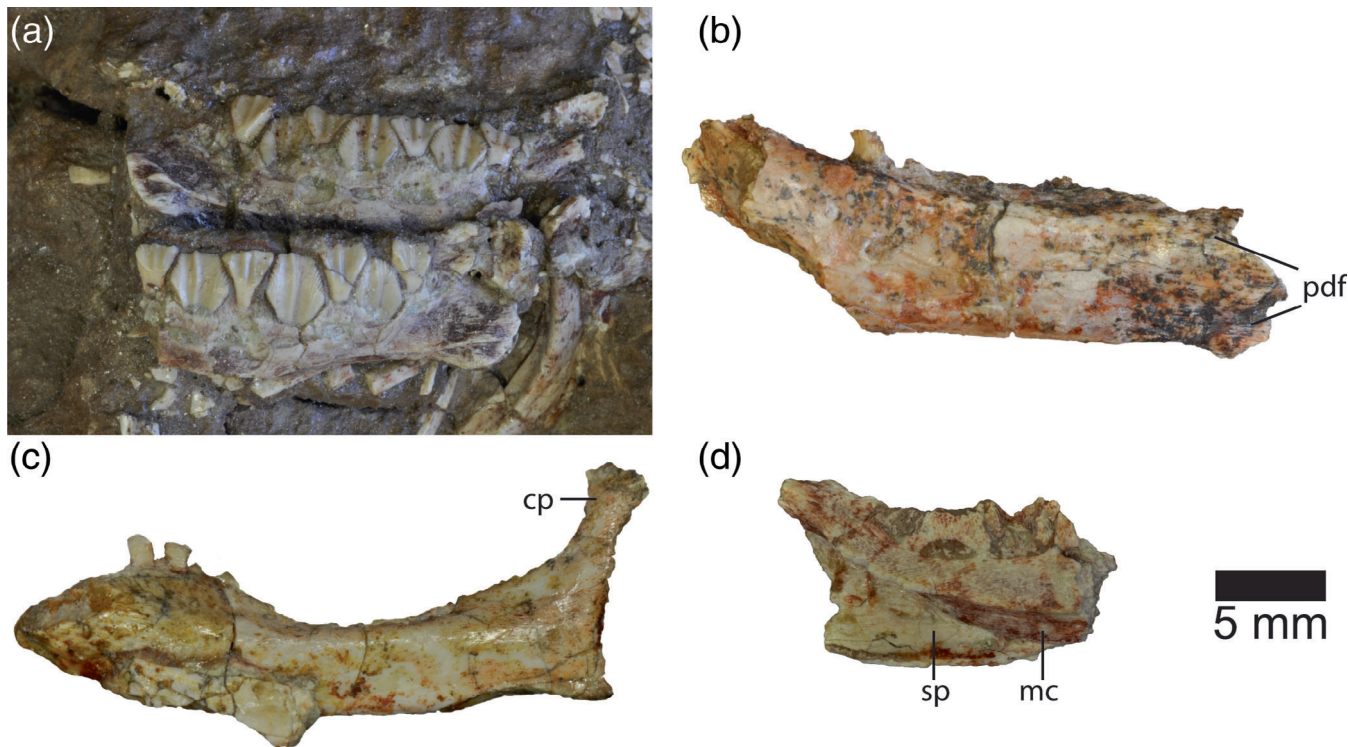


FIGURE 20 The dentaries of *Iyuku*. (a) Left (bottom) and right (top) dentaries, both in medial views, of AM 6150. (b) Partial right dentary of AM 6120 in lateral view showing a complete rostral end with facets for the predentary. (c) Partial left dentary of AM 6155 in lateral view showing a complete coronoid process. (d) Partial left dentary of AM 6052 in medial view showing a partial splenial in place over the Meckelian canal. cp, coronoid process; mc, Meckelian canal; pdf, predentary facet; sp, splenial

received the intermandibular portion of the caudoventral process of the predentary (Figure 20a). Behind this the ventromedial margin of the dentary bears a deep Meckelian sulcus that appears to have extended forward to reach the rear of the dentary symphysis (AM 6053, 6150). The Meckelian sulcus deepens caudally to occupy 60% of the depth of the dentary at the rear of the toothrow (AM 6052; Figure 20d). The dorsal margin of the sulcus continues to curves upwards to just beneath the dentary coronoid process. The Meckelian sulcus is flanked laterally by only a thin sheet of dentary bone, and dorsally by the tooth chamber.

The caudal dentary rises into a coronoid process immediately behind the last tooth (Figure 20c). The medial margin of the base of the coronoid process is in line with the rear of the last alveolus (AM 6052, 6153) and the toothrow does not pass medial to the coronoid process and the coronoid process is not offset laterally from the toothrow as it is in later-branching iguanodontians (e.g., *Mantellisaurus*, NHMUK R5764; *Protohadros*, SMU 74638). In lateral view, the coronoid process angles caudodorsally at approximately 30° from vertical and expands slightly rostrally at its distal tip, terminating well above the level of the toothrow (AM 6155). The angled coronoid process in *Iyuku* is similar to that of *Dryosaurus* (Galton, 1983) and *Dysalotosaurus*

(Hübner & Rauhut, 2010) but differs from the vertically orientated coronoid processes of later-branching iguanodontians (e.g., *Iguanodon*, IRSNB 1535; *Probactrosaurus*, Norman, 2002; *Protohadros*, SMU 74638). The caudal margin of the dentary is gently concave in lateral view where it articulates with the surangular and angular (Figure 20c).

Nine teeth are present in the dentary of AM 6053: seven large teeth are flanked by much smaller ones on either end of the toothrow. Seven large teeth are present in AM 6155 also, plus a tiny one in the front of the toothrow. The toothrows of AM 6053 and AM 6155 are both 19.7 mm in length. In 6150 (toothrow length 18.4 mm) seven large teeth are present and there appears to be a space for a small rostral tooth in the left dentary (Figure 20a). A small caudal tooth seems to be absent although its presence or absence is difficult to confirm.

7.11 | Dentary teeth

The dentary teeth are similar to those of the maxilla in many respects but differ in others (Figure 21). Well preserved, unworn dentary teeth are present in the collection. Tooth roots and crowns are curved medially and the crowns are asymmetrical.

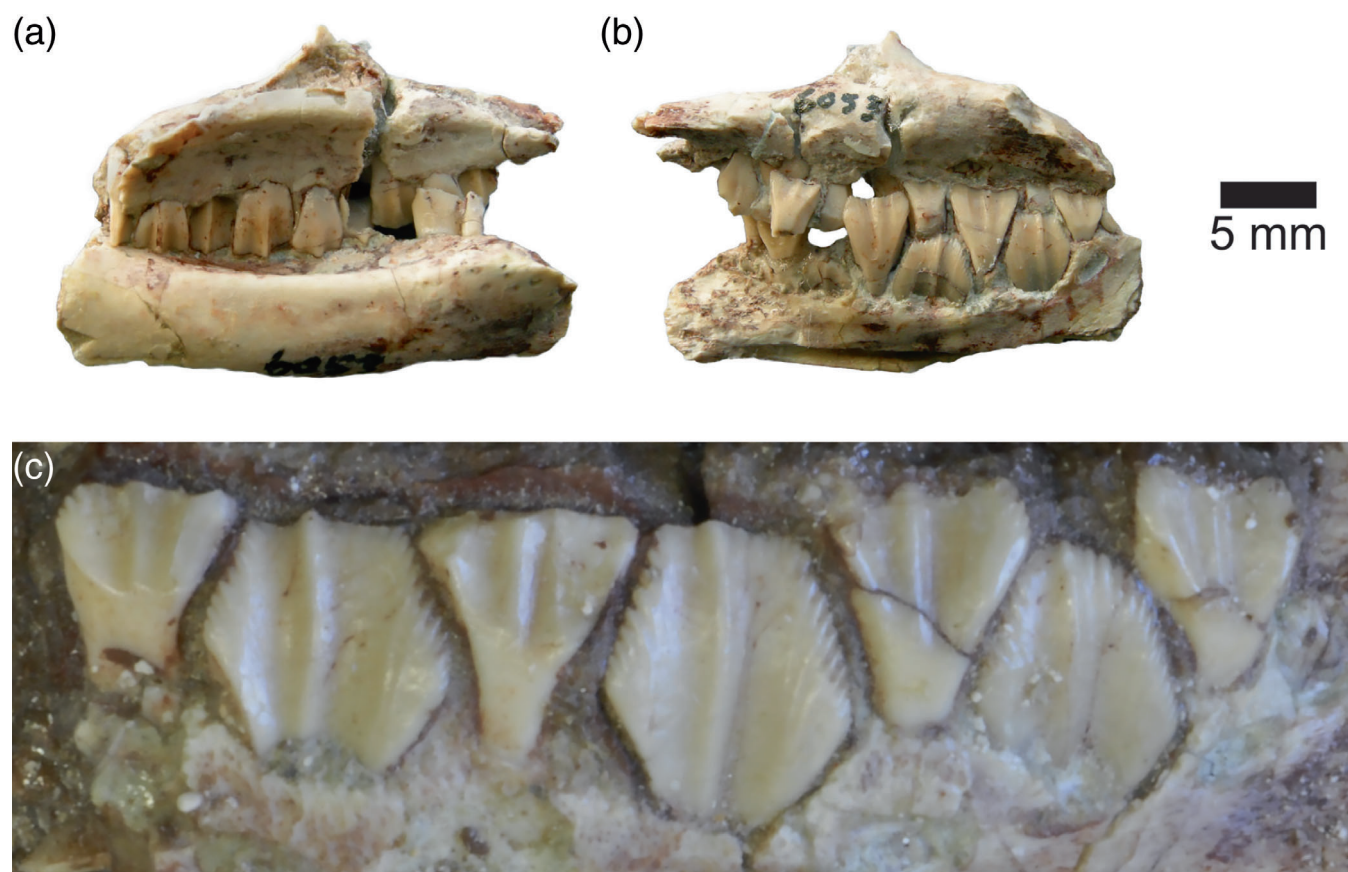


FIGURE 21 Dentary teeth of *Iyuku*. (a) Articulated right maxilla and dentary of AM 6053 in lateral view. (b) Articulated right maxilla and dentary of AM 6053 in medial view showing worn and unworn dentary teeth. (c) Dentary teeth in the left dentary of AM 6150 in medial view showing worn and unworn dentary teeth

The root is compressed mesiodistally but widens to the crown. The mesial and distal sides of the root near the crown are flattened. Deep V-shaped facets, widening towards the root, indent the mesial and distal sides of the base of the crown below its widest part. These facets accommodate the denticulate margins of the adjacent replacement tooth crowns along the tightly packed tooth-row. Each dentary tooth appears to have a single replacement tooth. The facet on the distal side of the crown extends slightly further toward the apex of the tooth than the mesial one, reflecting the asymmetry of the crowns.

Dentary tooth crowns are more heavily enameled on their ornamented lingual side and around the marginal denticles than on the labial surface. The crowns reach their widest point between one-half to one-third of the distance to their apex and the largest teeth are in the center of the dentary (Figure 21c). Dentary teeth possess a strong apical ridge that is offset slightly to the distal side of the crown so that the mesial portion of tooth is wider and bears a longer margin. Unlike the maxillary teeth, dentary teeth have one to three accessory ridges mesial to the apical ridge that continue down the face of the crown up to

or nearly up to the base of the crown. Occasionally there an accessory ridge also occurs on the narrower distal surface of the crown. These accessory ridges are less distinct than the apical ridge and connect to marginal denticles.

There are 10–16 marginal denticles along each side of the apical denticle; more occur on the broader mesial margin of the crown. Denticles only occur on the tooth margins distal to the widest part of the crown. The mesial portion of the crown is slightly longer than the distal portion. The denticulate margin of the distal crown is nearly straight from the apical denticle to the widest part of the crown. By contrast, the denticulate margin of the mesial crown extends nearly horizontally away from the apical denticle for a short distance (~five denticles), and in some teeth this margin is even slightly concave (e.g., AM 6053, Figure 21b), before abruptly turning rootward to mimic the angle of the distal crown. The apex of the mesial crown appears “squared off” relative to that of the distal crown. This nearly horizontal portion of the mesial margin overlaps the root of the preceding tooth in the magazine (Figure 21b). Thus the asymmetry of the apical ridge and denticular margin accommodates the close packing of the teeth. This morphology is very

similar to that of *Dysalotosaurus* (Janensch, 1955, Figure 14a,b), except that *Iyuku* lacks the fine subsidiary ridges on the mesial and distal crown of that taxon.

The lingual surface of dentary crown is gently convex mesiodistally, and is covered by an extremely thin layer of enamel, mirroring that of the maxillary crowns. A low, rounded ridge extends along the apicobasal length of the tooth crown on the unornamented labial surface, mirroring the apical ridge on the lingual side.

7.12 | Splenial

A small part of the splenial is preserved in AM 6053 as a very thin plate with a dorsoventrally curved dorsal margin (Figure 20d). All of its margins are eroded or broken. A portion of the splenial is preserved in place on the medial dentary in AM 6052 but lacks both its rostral and caudal extremity. The element tapers rostrally and deepens caudally as its dorsal margin curves caudodorsally to approach the coronoid process. The ventral margin appears straight. At the base of the coronoid process the splenial covers approximately three quarters of the depth of the dentary. The splenial appears to be restricted to the medial surface, although poor preservation of the ventral surface of AM 6053 makes this difficult to confirm.

7.13 | Surangular and angular

Two right surangulars (AM 6109, AM 6110) are exposed in lateral view (Figure 22). AM 6110 is nearly complete, and the rostral and caudalmost portions of AM 6109 are missing although the glenoid region is well preserved. AM 6109 also contains a small sliver of the angular. The margin of the external mandibular fenestra and contact with the dentary are missing or damaged on both specimens.

The ventral margin of the surangular is straight and bears a deep facet for the angular along nearly the entire margin. Below the retroarticular process the facet is primarily on the ventral surface. Rostral to this the facet moves onto the ventrolateral surface and deepens rostrally; a small portion of the angular is preserved in place in AM 6109 in the glenoid region (Figure 22b). At its maximum depth at the coronoid process the angular would have occupied approximately the lower 33% and the surangular the upper 67% of the postdentary depth, as in *Dysalotosaurus* (Hübner & Rauhut, 2010).

The articular surface of the glenoid is not exposed on either surangular. However, the surangular is constricted dorsoventrally where it would have contacted the articular. Immediately rostral to this the surangular rises into a

dorsally convex surangular process which forms a low rostrolateral wall to the glenoid fossa, as occurs in many ornithopods (e.g., *Iguanodon*, IRSNB 1535; *Jeholosaurus*, Barrett & Han, 2009). A rostrocaudally elongate surangular foramen is present at approximately the level of the jaw articulation and below and just rostral to the apex of the surangular lip (Figure 22). A surangular foramen is found in many ornithopods (e.g., *Hypsilophodon*, Galton, 1974; *Tenontosaurus*; Thomas, 2015) but is lost altogether in hadrosaurids. In early-diverging iguanodontians (e.g., *Tenontosaurus*; Thomas, 2015) the surangular foramen is positioned more rostrally and well in front of the articular. In other iguanodontians, the surangular foramen is positioned at or immediately rostral to the apex of the lip (e.g., *Mantellisaurus*, NHMUK R11521; *Protohadros*, SMU 74582).

Rostral to the surangular lip, the element rises steeply rostrodorsally to form a mediolaterally compressed plate that comprises a substantial portion of the coronoid process (AM 6110; Figure 22b). Although the rostral margin of the surangular is not perfectly preserved in AM 6110, it appears to be rostrocaudally broad and similar to that of some iguanodontians (e.g., *Zalmoxes*, Weishampel et al., 2003; *Tenontosaurus*, Thomas, 2015), but differing from the narrower margins of others (e.g., *Probactrosaurus*, Norman, 2002; hadrosaurs). No foramina pierce the rostral portion of the surangular,

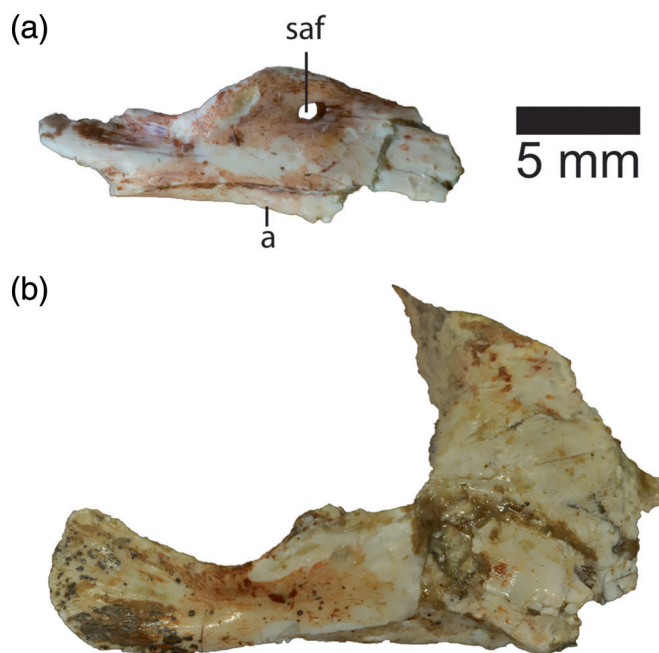


FIGURE 22 Surangulars of *Iyuku*. (a) Partial right surangular of AM 6109 with an open surangular foramen in lateral view with a small piece of the angular along its ventral margin. (b) Right surangular of AM 6110 in lateral view. a, angular; saf, surangular foramen

although damage to this area, particularly the rostroventral margin, would obscure such features.

The mediolaterally compressed retroarticular process of the surangular flares caudodorsally behind the glenoid region to approximately the height of the element at the apex of the surangular lip. Fine striae extend across the distal tip of the retroarticular process. The ventral surface of the retroarticular process is thickened and rounded where it meets the angular.

8 | AXIAL COLUMN

Despite their tiny size, isolated vertebral centra are common in the quarry. Articulated and well-preserved vertebrae and ribs are extremely rare, and only two centra with neural arches are known (AM 6034, AM 6066). In the most complete, partially articulated specimen preserved (AM 6150), the partial axial column is disarticulated and scattered; vertebral counts are not known for *Iyuku*. At least 70 disarticulated centra from the cervical, dorsal, sacral, and caudal series are present in the collection, primarily from very small juvenile individuals. Here we describe well-preserved representatives through the axial series.

8.1 | Cervical vertebrae

Two nearly complete cervical vertebrae are present in the collection. AM 6066 is a complete cervical vertebra from the cranial part of the series from a very small juvenile individual; this specimen is preserved in articulation with the neural arches of the preceding two cervical vertebrae. AM 6187 is a well-preserved, isolated cervical centrum from the caudal portion of the series from a sub-adult individual (Figure 23).

In the larger AM 6187 the centrum is slightly shorter craniocaudally than its maximum width and is dorsoventrally compressed (height is 50% length). In lateral view the rostral and caudal articular faces both lean slightly forward, as is typical among ornithopods for cervicals closest to the dorsal series (e.g., *Tenontosaurus*, *Iguanodon*; Figure 23). The vertebra is amphicoelus; the cranial articular face is slightly concave whereas the caudal articular face is more deeply concave (Figure 23a,b). The parapophysis is dorsoventrally compressed and occupies the cranial one-third of the centrum. In lateral view the parapophyses are located slightly above the midpoint of the articular face (Figure 23a,b). The articular surface of the parapophysis is oriented craniolaterally. In ventral view the centrum bears a very broad, rugose keel that extends from the cranial articular face

approximately two-thirds of the way down the centrum (Figure 23d). Between keel and parapophysis the lateral surfaces of the centrum is concave (as in *Iguanodon*, Norman, 1980).

In dorsal view the articular surfaces for the neural arches are hourglass-shaped and closely approach each other along the midline near the midpoint of the centrum's length (Figure 23c). A pair of craniocaudally elongate neurovascular foramina pierce the base of the neural canal where the neural arch articulations most closely approach one another. The neural arch articular surfaces are oriented dorsolaterally at 45° along the entire centrum. The neural arch articular surfaces curve craniolaterally and also expand in width to cover the entire dorsal surface of the diapophyses.

No cervical ribs have been identified.

8.2 | Dorsal vertebrae

A well-preserved dorsal centrum of a sub-adult individual was recovered from the quarry (AM 6031; Figure 24). The centrum is weakly amphicoelus and lacks parapophyses (Figure 24a). The cranial articular face is nearly equidimensional, being very slightly dorsoventrally compressed. This compression is more pronounced on the caudal articular face (Figure 24b,c). The centrum constricts both dorsoventrally and mediolaterally towards its midpoint to 70% of the cranial articular face. The ventral surface is rounded and lacks a keel (Figure 24g).

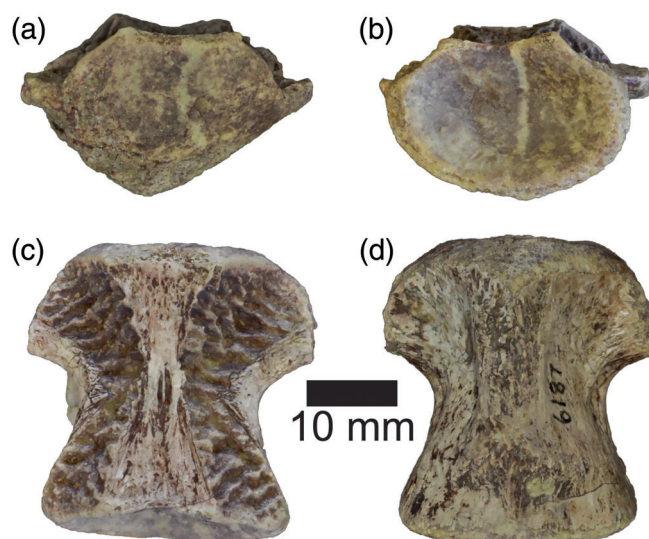


FIGURE 23 Cervical vertebral centrum from the caudal portion of the series of *Iyuku*, AM 6187. (a) Rostral view; (b) caudal view; (c) dorsal view, cranial end up; (d) ventral view, cranial end up

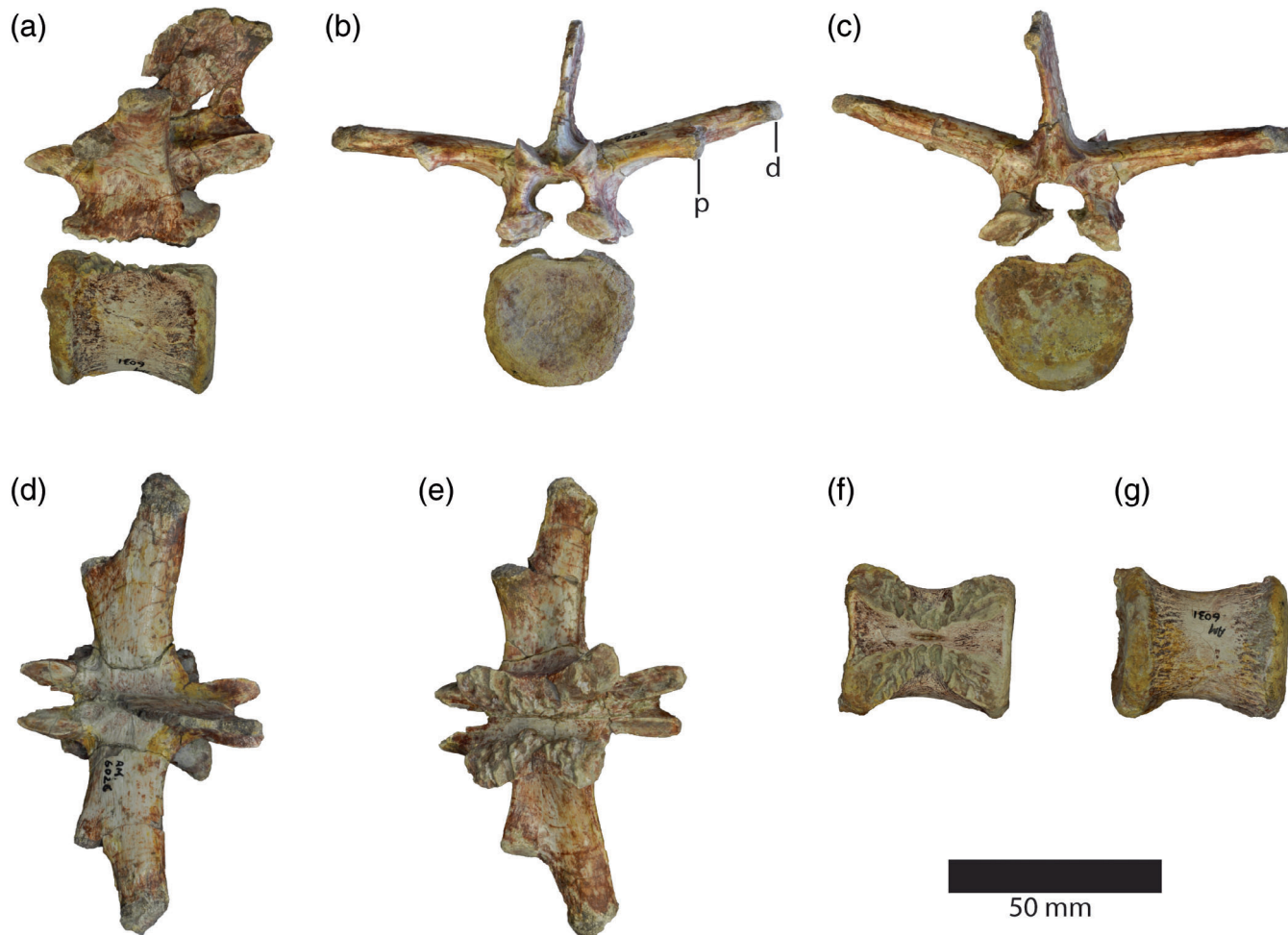


FIGURE 24 Dorsal vertebral centrum (AM 6031) and neural arch (AM 6026) of *Iyuku*. (a) Left lateral view of centrum and arch. (b) Cranial view of centrum and arch. (c) Caudal view of centrum and arch. (d) Dorsal view of arch, cranial to the left. (e) Ventral view of arch, cranial to the left. (f) Dorsal view of centrum, cranial to the left. (g) Ventral view of centrum, cranial to the left. d, diapophysis; p, parapophysis

As with the cervical centrum, the rugose articular facets for the neural arches extend the entire length of the dorsal centrum (Figure 24f). In dorsal view they are hourglass-shaped, closely approaching each other at their midpoint. The narrow base of the neural canal exposed between the articular facets at this midpoint is deeply incised by an elongate, narrow neurovascular foramen (Figure 24f).

One isolated dorsal neural arch from a sub-adult individual was also recovered from the quarry (AM 6026; Figure 24). Although this arch does not articulate perfectly with the AM 6031 centrum (described above) the articular facets of the arch and centrum are the same length, width, and shape, and the articular surfaces on the neural arch mirror those on the centrum. These two specimens may be from the same vertebra (slight distortions negating their firm articulation) or possibly from adjacent vertebrae.

When AM 6026 and 6031 are articulated, the pre- and postzygapophyses extend well beyond the margins of the centrum and would have overlapped adjacent centra. The neural canal is oval, being 30% wider than tall. The pre- and postzygapophyseal facets are ovate and cranio-caudally elongate to at least twice as long as they are wide; the prezygapophyses are also somewhat pointed cranially. The surfaces of both pre- and postzygapophysal facets are angled about 45° from horizontal, with the prezygapophyseal facets facing dorsomedially and postzygapophyseal facets oriented ventrolaterally.

The blade-like neural spine is slightly shorter than the maximum height of the centrum. The spine is cranio-caudally broad and equals the craniocaudal length of the laminae; its base extends the entire length between pre- and postzygapophyses (Figure 24a). The spine thickens slightly mediolaterally only at its tip. The caudal margin of the spine is slightly concave in lateral view and at its

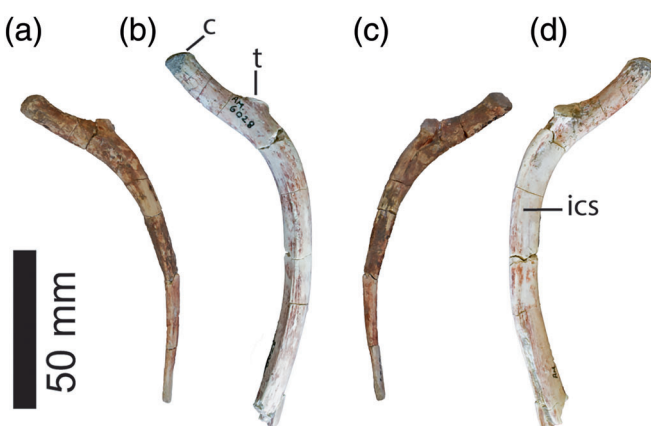


FIGURE 25 Dorsal ribs of *Iyuku*. (a) AM 6027 in cranial view. (b) AM 6028 in cranial view. (c) AM 6027 in caudal view. (d) AM 6028 in caudal view. c, capitulum; ics, intercostal sulcus; t, tuberculum

distalmost tip extends caudally as far as the terminus of the postzygapophysis.

The robust, dorsoventrally compressed transverse processes extend across nearly the entire craniocaudal width of the laminae (Figure 24d,e). The transverse process is oriented 30° above horizontal on the left side but only approximately 15° on the right. The transverse process is directed laterally from the arch in dorsal view (Figure 24d,e). The parapophysis is located on the cranial margin of the transverse process approximately half of the way to the distal end (Figure 24d,e). Based on parapophyseal position this neural arch is likely from a mid-dorsal vertebra. The parapophysis is oval in outline with a nearly flat articular surface that is oriented ventrolaterally. The diapophysis is also oval in outline but with a convex articular face oriented caudolaterally. It is slightly larger than the parapophysis and more compressed dorsoventrally.

8.3 | Dorsal ribs

Four partial (AM 6028, 6029, 6035) to complete (AM 6027) dorsal ribs from a sub-adult were found in the quarry. In all, six left and one right dorsal ribs from the cranial to mid-dorsal region can be identified, as the capitulum and tuberculum are well separated from one another on all specimens (Figure 25). They are all similar in size to one another, and to the dorsal neural arch (AM 6026) described above, and may pertain to the same or similar sized individuals.

In all ribs the capitulum ends in a convex, nearly round facet set on a long nearly round stalk that becomes

compressed along its dorsal margin as it nears the tuberculum. The tubercular facet is nearly flat and oriented caudomedially relative to the shaft of the rib and capitular stalk. The shaft of the rib is compressed mediolaterally with narrow cranial and caudal margins. The internal aspect of the caudal margin bears a sulcus for the intercostal neurovasculature (e.g., AM 6029). The shoulder of the rib is concave caudomedially; this concavity narrows distally to become the intercostal sulcus. In AM 6027, a short complete rib, the distal shaft tapers to a blunt end, and the capitular stalk is 28% the length of the shaft.

8.4 | Sacral vertebrae

Two sacral centra from sub-adult individuals come from the quarry, including one with a partial right neural arch (AM 6186 and AM 6034, respectively; Figure 26). Two articulated but unfused sacral vertebral centra are exposed in dorsal view in AM 6150.

AM 6064 appears to be a sacrodorsal vertebra: the caudal end of the centrum expands 22% over the cranial centrum and bears large facets for the first sacral rib, as in other ornithopods (e.g., *Jeholosaurus*, *Tenontosaurus*, *Barilium*, *Iguanodon*). Overall the centrum is dorsoventrally compressed, constricted centrally, then expands greatly to meet the first sacral centrum (Figure 26d,e). The cranial articular face of centrum is slightly concave from side to side while the caudal articular face is flat. The articular facet for the first sacral rib facet occupies the upper half of the caudal 25% of the centrum (Figure 26c). This rugose rib facet has a concave surface that is oriented caudolaterally and extends behind the caudal articular face of the centrum. The ventral centrum is rounded and lacks any evidence of a keel or sulcus (Figure 26e).

The neural canal is relatively wider than that of the dorsal centrum (AM 6031) although neural arches still pinch inward toward the center of the centrum. A slight depression occurs along the base of the neural canal at the midpoint of the centrum, but appears to lack neurovascular foramina like those in the cervical and dorsal vertebrae.

The right neural arch preserves the lamina, prezygapophysis, and part of base of the neural spine and transverse process. The lamina arises from the entire length of the centrum but rapidly narrows craniocaudally (Figure 26a). The prezygapophysis is small and does not extend beyond the cranial margin of the centrum. The prezygapophyseal facet is oval and 25% longer axially than wide. The facet is oriented dorsomedially about 20° above horizontal.

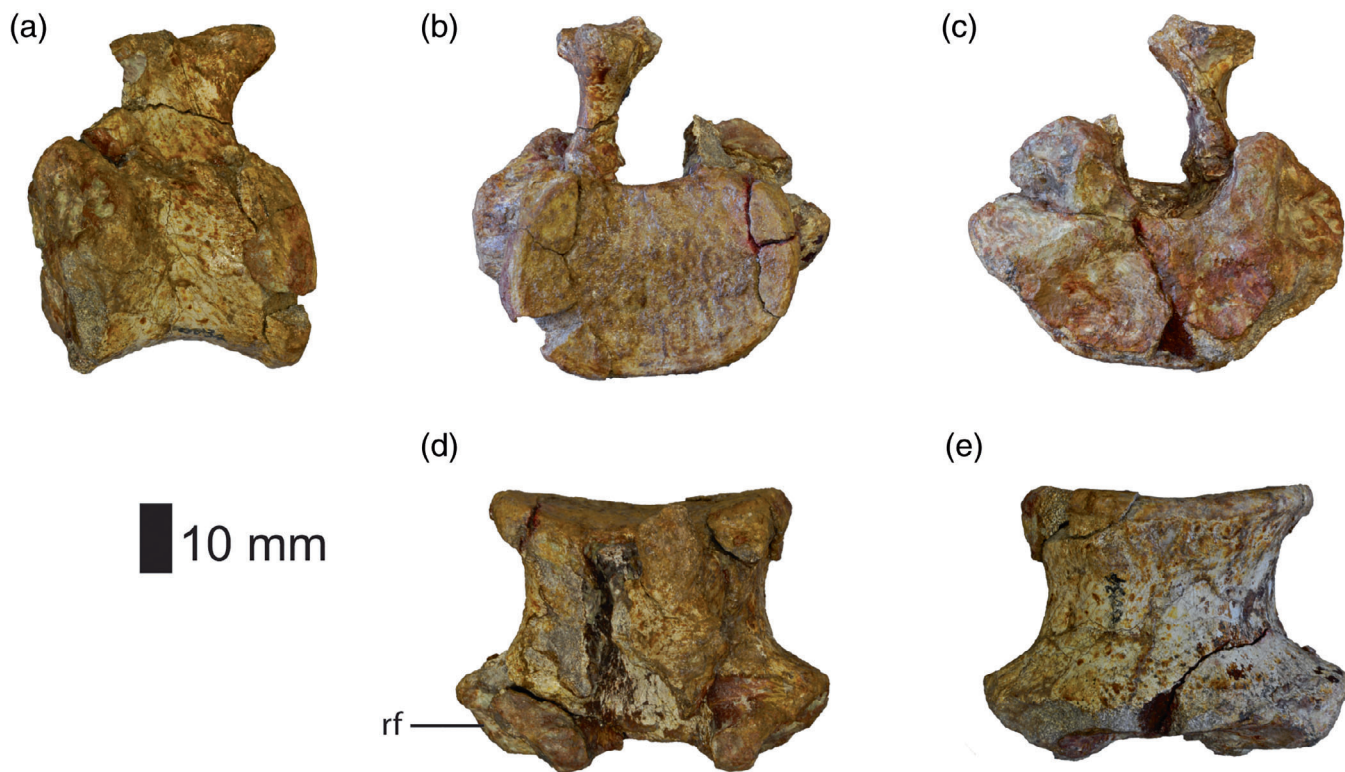


FIGURE 26 Sacral vertebra of *Iyuku*, AM 6034, in (a) right lateral view; (b) cranial view; (c) caudal view; (d) distal view, cranial end up; (e) ventral view, cranial end up. rf, rib facet

The two centra in AM 6150 are missing their arches. The centra are wider than they are long, and appear hollow. No other morphology can be discerned.

No sacral ribs have been recognized.

8.5 | Caudal vertebrae

Caudal vertebrae are represented by isolated centra from small juveniles (e.g., AM 6070 collection, AM 6088 collection; AM 6150, Figure 27a). The position of these isolated centra in the tail cannot be positively identified. The elongate caudal centra were laterally compressed with a sulcus of varying depth and width on the ventral surface. A small foramen is often present in the base of the neural canal. The cranial and caudal articular faces are slightly concave, making the vertebrae amphicoelous.

One chevron has been identified in AM 6150 (Figure 27b). Its position in the tail cannot be ascertained. The chevron spine is straight and appears to taper distally although it may not be complete. Proximally the left and right articular facets are separate and do not meet above the large haemal canal.

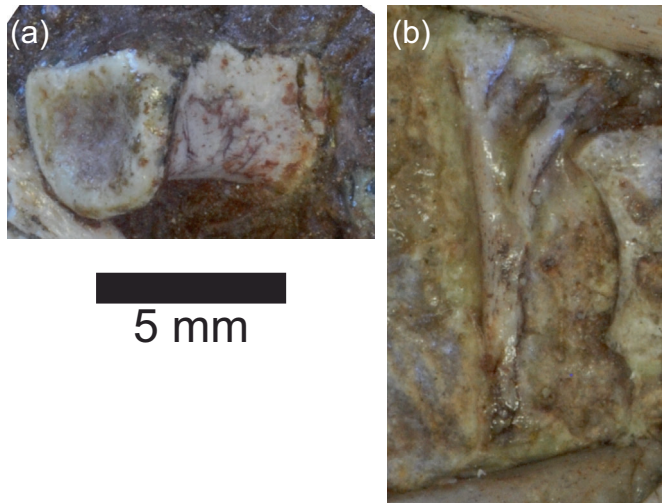


FIGURE 27 Caudal vertebrae of *Iyuku*. (a) Isolated caudal vertebra of AM 6150. (b) Isolated chevron of AM 6150

9 | PECTORAL GIRDLE AND FORELIMB

No articulated forelimb material is known, and no coracoid or manus elements have been positively identified.

The holotype specimen (AM 6150) preserves both scapulae but no other forelimb material. Proportional information between forelimb elements, and between the forelimb and hind limb (other than the scapula) are not possible.

9.1 | Scapula

One complete left (AM 6063) and three partial left (AM 6176, AM 6175, AM 6102) scapulae are known from isolated materials, and both scapulae are present in AM 6150 (Figure 28). The scapula in AM 6150 is 69% the length of the femur.

The scapula is well curved to conform to the surface of the ribcage, especially proximally where it curves craniomedially towards the sternum (Figure 28c,d). The acromion process only projects above the coracoid articulation a short distance and bends laterally to form a scapular spine that makes the lateral surface of the articular end appear concave. The coracoid articular facet is somewhat mediolaterally compressed, narrows towards the glenoid, and occupies 60% of the depth of the proximal scapula (AM 6063). The concave scapular glenoid narrows slightly as it approaches the coracoid articulation.

The medial surface of the proximal scapula is slightly convex except for a broad, shallow sulcus that bisects the proximal end from the coracoid articulation back towards the blade for a short distance, as it does in some ornithopods (e.g., *Convolosaurus*, Andrzejewski et al., 2019; *Camptosaurus*, USNM 4282) (Figure 28b).

In lateral view, the dorsal margin of the scapula is nearly straight, with only a slight flare to the small acromion process in some specimens (e.g., AM 6152, AM 6063; Figure 28a,b,f), and a slight dorsal flare to the distal blade. A straight dorsal scapular margin is also seen in other iguanodontians (e.g., *Tenontosaurus*, Forster, 1990; *Iguanodon*, Norman, 1980) contrasting to more primitive ornithischians and ornithopods with large dorsally flaring acromion processes (e.g., *Haya*, Makovicky et al., 2014; *Anabisetia*, Coria & Calvo, 2002). The scapular blade constricts to a neck 45% the depth at the proximal end through the deep incision of the ventral margin behind the glenoid. Behind the constricted neck the ventral margin of the scapula flares to the distal end so that the distal scapular blade is notably deeper than the articular end. The distal end of the scapular blade is mediolaterally compressed, and its most distal point is at or near the ventral corner of the blade. There also appears to be a slight dorsal flare to the distal scapular blade (Figure 28f). The

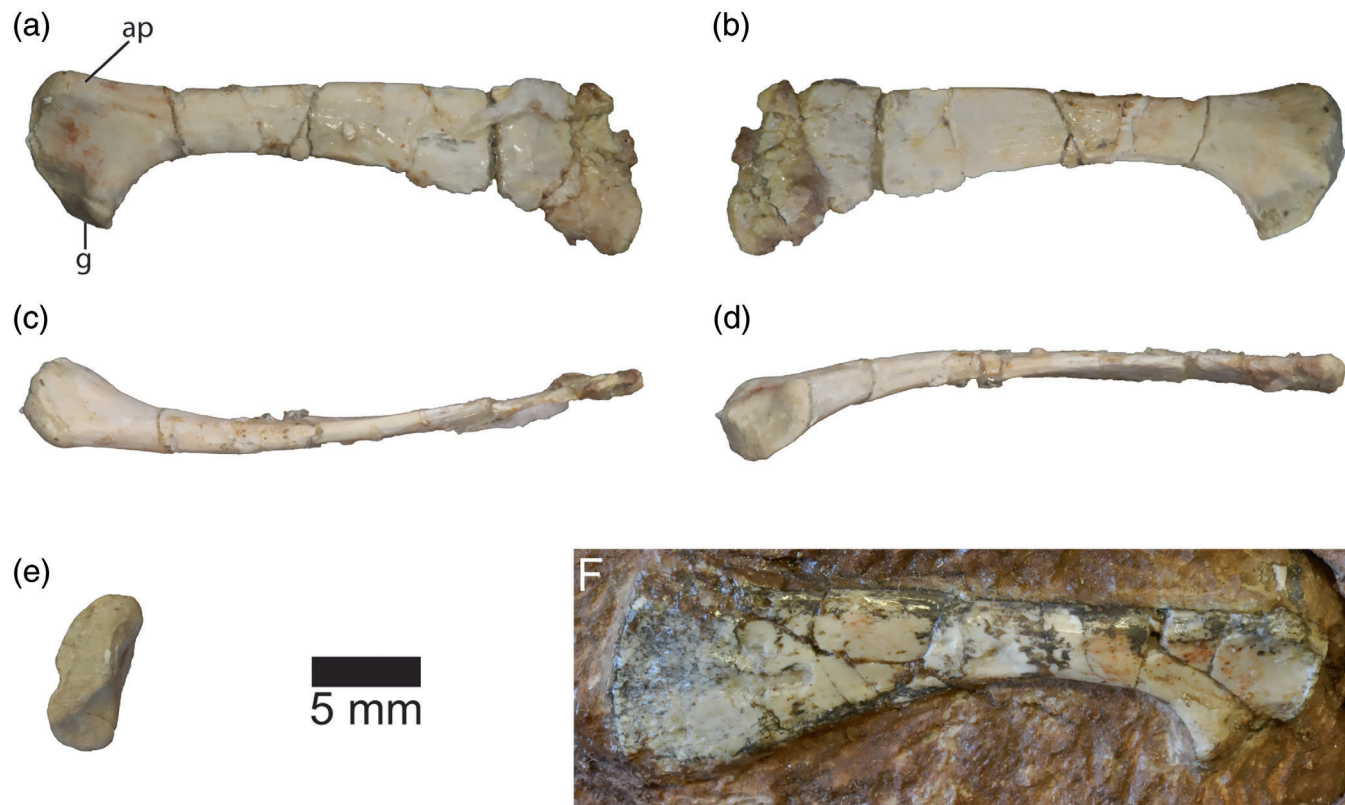


FIGURE 28 Scapulae of *Iyku*. Left scapula of AM 6063 in (a) lateral; (b) medial; (c) dorsal; (d) ventral; (e) articular views. (f) Right scapula of AM 6150 in lateral view. ap, acromion process; g, glenoid

shape of the scapular blade closely resembles that of many early-branching iguanodontians (e.g., *Tenontosaurus*, Forster, 1990; *Zalmoxes*, Weishampel et al., 2003) but unlike the modest, more eqidimensional distal flare of later-branching taxa (e.g., *Iguanodon*, Norman, 1980; *Proabactrosaurus*, Norman, 2002).

9.2 | Sternal plate

A single, delicate left sternal plate is present in the collection (AM 6067; 19.6 mm in total length; Figure 29). It has the derived “hatchet-shape” of styracosternan iguanodontians in possessing a handle-like caudolateral process (e.g., *Iguanodon*, *Lurdusaurus*, hadrosaurids) rather than the reniform shape of more early-branching ornithopods (e.g., *Camptosaurus*, *Tenontosaurus*, *Hypsilophodon*, *Dryosaurus*). However, Poole (2015) found the ossification of a caudolateral process to be homoplastic in iguanodontians, evolving at least three times within the clade (*Iyuku*, *Macrogyphosaurus*, Styracostera), as well as independently in pachycephalosaurs (Maryanska & Osmólska, 1974).

The caudolateral process of the sternal plate is gracile and nearly straight with only a slight medial curvature along the lateral margin. The process is thick and rounded along its lateral margin, but thins to a more compressed edge medially. It thickens dorsoventrally and expands slightly mediolaterally to its distal terminus to end in a rounded knob.

The cranial end of the sternal plate expands into a broad, flat body that occupies more than half (56%) the total length of the element, a much larger proportion than seen in many ornithopods (e.g., *Iguanodon*) (Figure 28b,c). Its internal (dorsal) surface is gently concave, while the external (ventral) surface is nearly flat. The straight, thick lateral margin of the sternal body is flattened and canted slightly ventrally, and mirrors the caudolateral process in its thickness (Figure 29a). Medial to this thickened lateral margin the sternal body is uniformly thin. In dorsal (internal) view, the medial margin curves sharply medially from the caudolateral process, then turns cranially in a broad convex arc that meets the craniomedial corner of the element. The margin of this broad convex arc is rugose and thickened dorsoventrally relative to the body of the sternal plate; it is thickest at its cranial and caudal corners. This rugose margin contacted the contralateral sternal plate.

9.3 | Humerus

Four complete right (AM 6054, 6173, 6094), one complete left (AM 6095), a proximal right (AM 6096), and a distal right (AM 6097) humerus are present in the collection, representing at least five juvenile individuals (Figure 30).

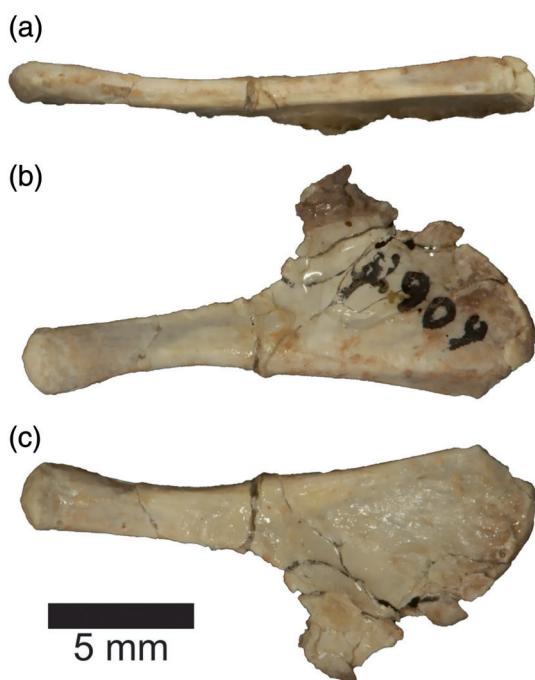


FIGURE 29 Left sternal plate of *Iyuku*, AM 6067, in (a) medial; (b) dorsal; (c) ventral views



FIGURE 30 Right humerus of *Iyuku*, AM 6054, in (a) lateral; (b) cranial, (c) caudal views. The distal end of the humerus is poorly preserved. dpc, deltopectoral crest; hh, humeral head

The complete humeri range from 26.7 (AM 6054) to 33.1 mm (AM 6094) in length.

The humerus is very slender and the proximal and distal ends are only modestly expanded (Figure 30b,c). In proximal view the humerus is slightly sinuous, curving back to the medial margin. The humeral head is rounded and centered on the caudal surface of the proximal end, but is not well preserved in any of the specimens. Distal to the proximal end the humerus narrows slightly to the low and poorly defined deltopectoral crest. The small, distally-tapering deltopectoral crest bends to the cranial aspect of the lateral margin of the humerus. A similar tapering deltopectoral crest is seen in some ornithopods (e.g., *Iguanodon*), but differs from the robust and well-defined crests of others (e.g., *Hypsilophodon*, *Tenontosaurus*). The distal corner of the deltopectoral crest is located 40% of the way down the humerus. In *Tenontosaurus*, the deltopectoral crest also occupies 40% of humeral length in juveniles, but extends to 54% of humeral length in adults (Forster, 1990). The distal extent of the crest in adults may therefore have been further down the humerus in *Iyuku*.

Distal to the deltopectoral crest the humeral shaft is compressed craniocaudally and curves gently cranially to the distal condyles. The distal end is also compressed craniocaudally and its long axis is oriented about 40° lateral to the proximal expansion. The distal condyles flare mediolaterally but not as far as the proximal end. The cranial surface of the distal end is shallowly concave, forming a very broad and shallow flexor sulcus. On the caudal surface there is a well-defined and moderately deep olecranon fossa bordered by a blunt medial and sharper lateral epicondylar ridge. In distal view, the medial condyle is 18% deeper craniocaudally than the lateral condyle. The medial condyle exceeds the lateral condyle in mediolateral width as well, and extends further caudally than the lateral condyle, making its epicondylar ridge bordering the olecranon sulcus more prominent. The medial and lateral sides of the condyles are fairly flat, and the distal articular surfaces of the condyles are slightly convex. There is a shallow intercondylar sulcus.

9.4 | Ulna

Two proximal left ulnae have been found in Kirkwood Quarry. AM 6101 is a small, well-preserved fragment from a small juvenile (craniocaudal width 5.0 mm) and preserves approximately the proximal one-third of the ulna (Figure 31d–f). AM 6046 is a poorly preserved, eroded specimen from a subadult individual (Figure 31a–c). The olecranon process is very low and rounded, rising only slightly

above the level of the short coronoid process. The medial surface of the ulna is flat and there is a small radial process extending laterally from the proximolateral ulna. A blunt ridge extends distally from this process down the shaft, giving it a sub-triangular shape in cross-section (Figure 31c).

9.5 | Radius

One complete, well-preserved right radius is present in the collection (AM 6172). The gracile shaft is nearly straight except for a slight medial curve at its distal end (Figure 32a,b). The proximal end is expanded in all directions from the shaft and is twice as wide craniocaudally than the shaft. In proximal view the radial head appears oval and slightly mediolaterally compressed, narrowing caudally (Figure 32c). The articular surface is only slightly convex. The distal end is also expanded craniocaudally to slightly less than twice its mediolateral width, and extends further cranially than caudally from the shaft. In distal view, the distal radius is subtriangular with the apex pointing caudally (Figure 32d). The caudo-medial surface of the distal radius is flattened to articulate with the distal ulna.

10 | PELVIC GIRDLE AND HIND LIMB

The hindlimb contains the largest and most robust elements in the postcranial skeleton, and femora and tibiae are particularly well represented in the quarry sample. The tibia of AM 6150 easily exceeds the femur in length by 19%. However, elongation of the tibia relative to the femur in juveniles has been reported for other ornithopods, suggesting that hindlimb proportions are ontogenetically controlled (e.g., Dodson, 1980; Weishampel et al., 2003). Other ontogenetic changes are known in the hindlimbs of some ornithopods. For example, in *Zalmoxes* the anterior trochanter of the femur becomes more prominent and the fourth trochanter becomes more distally placed through ontogeny, while the cnemial crest of the tibia becomes proportionally larger (Weishampel et al., 2003). A small cnemial crest in juvenile specimens is also reported for *Dryosaurus* (Carpenter, 1994). Dilkes (2001) found that in *Maiasaura*, the fourth trochanter of the femur becomes relatively larger through ontogeny, while femoral circumference is negatively allometric. In the tibia of *Maiasaura*, all dimensions are isometric, except the circumference, which becomes proportionally smaller through ontogeny (Dilkes, 2001).

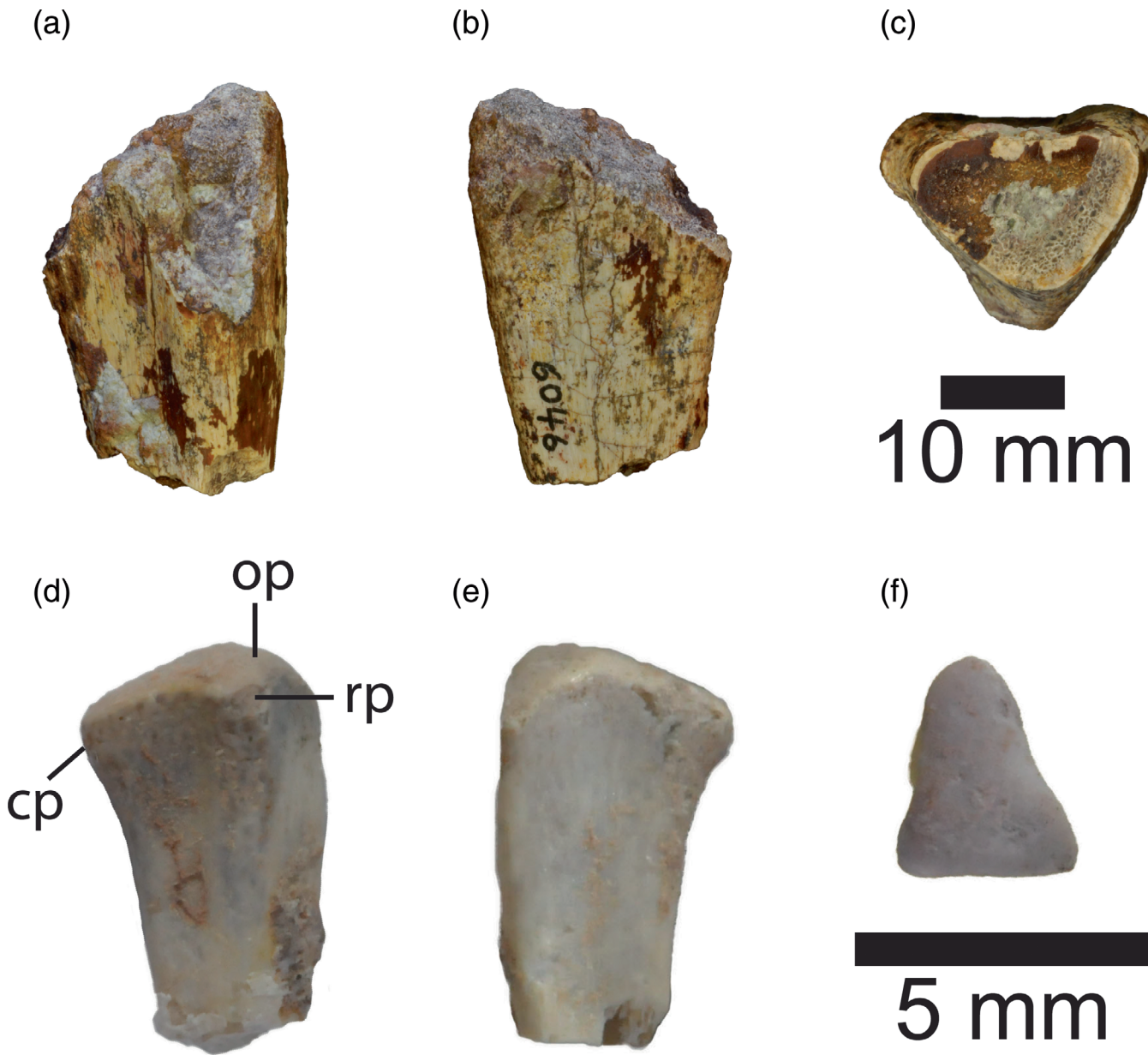


FIGURE 31 Proximal ulnae of *Iyuku*. Partial proximal left ulna of AM 6046 in: (a) lateral; (b) medial; (c) distal views. Proximal left ulna of AM 6101 in (d) lateral; (e) medial; (f) proximal, cranial end up, views. Five millimeters scale bar for d–f; 10 mm scale bar for a–c. cp, coronoid process; op, olecranon process; rp, radial process

10.1 | Ilium

Both ilia are preserved in AM 6150 and exposed in lateral view only; no other ilia are known (Figure 33). The right ilium is complete but the left ilium is missing its postacetabular process.

The substantial preacetabular process comprises 40% of the total length of the ilium. It curves gently craniocentrally and is 57% the depth of the iliac body over the acetabulum. It maintains its depth for its entire length. The tip of the preacetabular process ends at approximately the same level as the dorsalmost extent of the

acetabular rim. The distal end of the preacetabular process is not perfectly preserved on either side but is more complete on the left, and narrows substantially relative to the rest of the process. On both sides, the preacetabular process has a concave lateral surface and the dorsal margin is slightly everted along its length.

The dorsal margin of the ilium is nearly straight in lateral view and slightly everted laterally at least as far back as the center of the acetabulum, giving the lateral surface of the body also a slightly concave appearance. The acetabulum is shallowly embayed (20% the total depth of ilium) and craniocaudally narrow (12% total

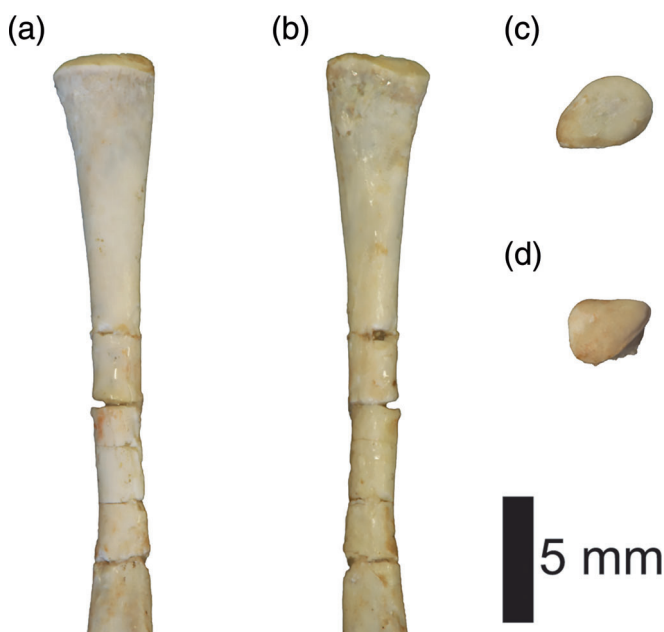


FIGURE 32 Right radius of *Iyuku*, AM 6172, in (a) lateral; (b) medial; (c) proximal; (d) distal views

length of ilium). The short pubic peduncle extends cranioventrally from the iliac body, and flares slightly laterally at its distal end. Its distal articular surface is not exposed. The short ischial peduncle is craniocaudally broad, equaling or even exceeding the acetabulum in width. It terminates in a flat ventral surface that extends distally to the same level as the pubic process. There is no antitrochanter developed on its lateral surface as occurs in other ornithopods (e.g., *Iguanodon*, *Dysalotosaurus*, *Jeholosaurus*, hadrosaurids), although this may be due to the early ontogenetic stage of the individual.

The postacetabular process occupies 32% of the length of the ilium and is dominated by an extremely large, broad brevis shelf that widens considerably towards its caudal limit. The caudal margin of the brevis shelf is straight and oriented mediolaterally. The shelf at this point is horizontal; its width is 40% the total length of the postacetabular process. In lateral view the ventral margin of the brevis shelf angles caudodorsally to terminate nearly at the dorsal margin of the ilium. A ridge on the lateral surface of the ilium extends from the caudal brevis shelf forward across the postacetabular process to end above the ischial peduncle. The ilium of *Iyuku*, with its extremely broad and dorsally angled brevis shelf, is similar to that of many iguanodontians (e.g., *Dryosaurus*, *Iguanodon*, *Camptosaurus*), in contrast to the deep

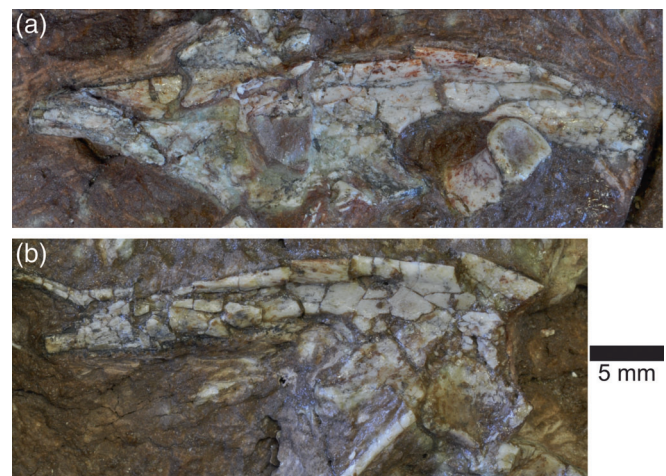


FIGURE 33 Ilium of the holotype of *Iyuku*, AM 6150, both in lateral view. (a) Right ilium; (b) left ilium, postacetabular process missing

postacetabular processes and nearly horizontal, narrow brevis shelf of others (e.g., *Tenontosaurus*, *Jeholosaurus*, *Hypsilophodon*).

10.2 | Pubis

Both pubes are present in AM 6150; the distal end of the right prepubis is partially covered by the right tibia but is either broken off or unossified on the left pubis. The postpubic rods are missing only their very distal tips or may have been unossified (Figure 34a,b). A partial left pubis from a larger subadult specimen (AM 6032) was also recovered from the quarry, and is missing the distal end of the prepubic process and the entire postpubic rod (Figure 34c,d).

The pubis is very gracile. The iliac facet is large, concave, faces caudolaterally, and covers the entire proximal part of the pubic body in AM 6150 (Figure 34a). The prepubic process is dorsoventrally narrow and extends nearly straight rostrally. There is a long, rounded process or tubercle arising from the ventrolateral margin of the base of the prepubic process (Figure 34a,c,d). In the subadult (AM 6032) this tubercle is larger than that of AM 6150 and hosts a well-developed rugosity on its lateral margin, possibly for the insertion of abdominal musculature. A similar morphology and rugosity is present in *Tenontosaurus tilletti* (Forster, 1990) although in that taxon the process is positioned further cranially on the prepubis. The prepubic process is slightly laterally compressed and appears to maintain its depth along most of its length. The prepubis has a slight dorsoventral expansion towards its distal end in the larger AM 6032. The lack of a pronounced distal expansion is seen among

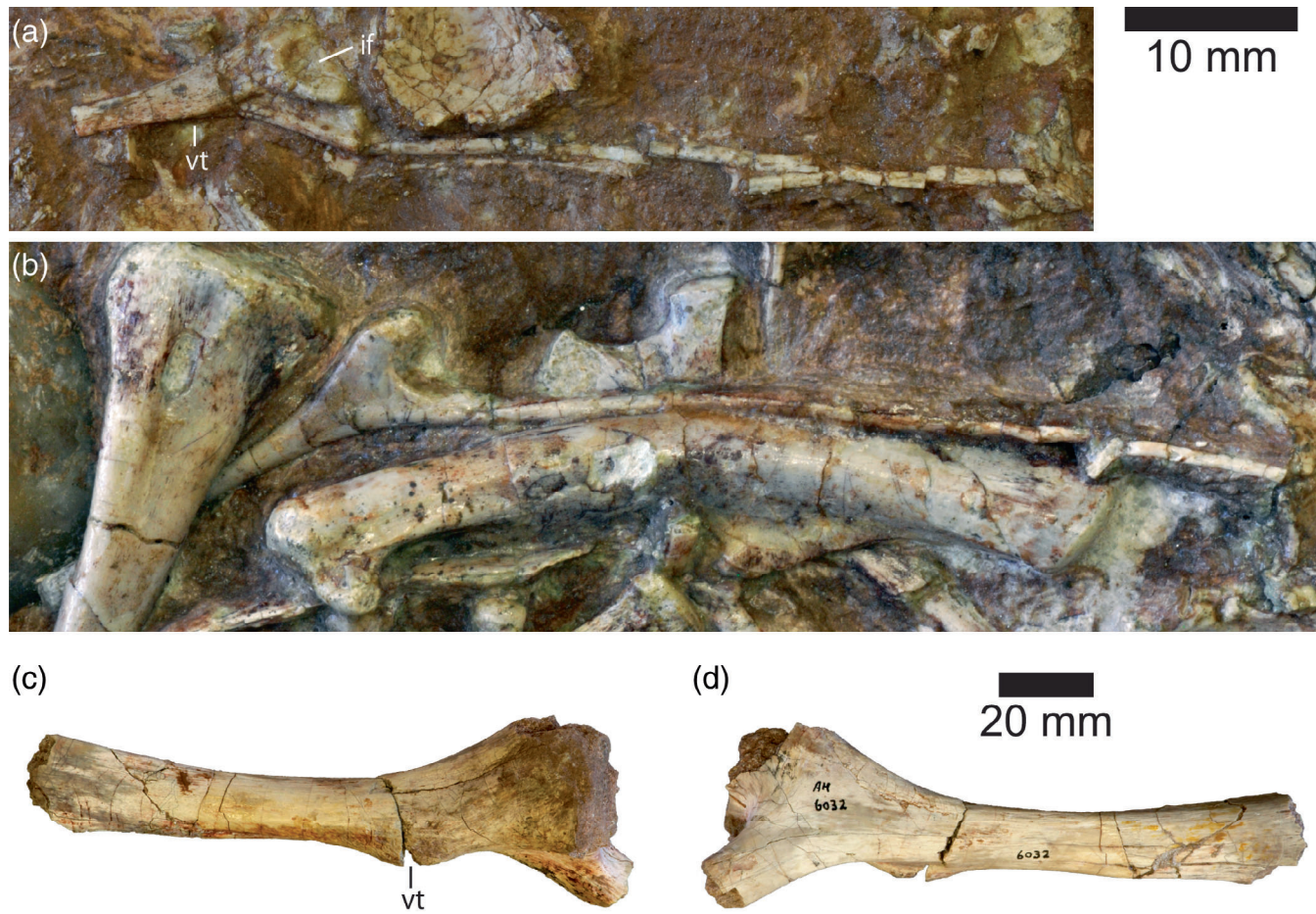


FIGURE 34 Pubes of *Iyuku*. (a) Left pubis of AM 6150 in lateral view. (b) Right pubis of AM 6150 in medial view. (c) Left pubis of AM 6032 in lateral view, postpubic rod missing. (d) Left pubis of AM 6032 in medial view, postpubic rod missing. if, iliac facet; vt, ventral tubercle

non-ankylopollexian ornithopods (e.g., *Tenontosaurus*, *Dryosaurus*, *Dysalotosaurus*), and differs from the broad distal expansions of ankylopollexians (e.g., *Iguanodon*, *Ouranosaurus*, hadrosaurids). In the sub-adult specimen (AM 6032) the pubis is slightly dorsoventrally compressed (13% wider than high) immediately in front of the ventral process. Distal to this, the blade becomes increasingly laterally compressed and begins to flare dorsoventrally. At the end of the preserved portion (the distal tip is missing) the blade is twice as tall as it is wide. A rod-shaped or dorsoventrally flattened prepubis is found in many ornithopods, such as *Dysalotosaurus* and *Hypsilophodon*. Ankylopollexians have prepubes that are mediolaterally compressed along their entire length (e.g., *Iguanodon*, *Ouranosaurus*, hadrosaurids), as does at least one more basal ornithopod (*Convolosaurus*). *Iyuku* appear to be intermediate in morphology. No distal flare is observed in AM 6150 although the prepubes are not complete (Figure 34a,b).

The postpubic rod arises from the ventromedial margin of the pubic body, and is directed slightly medially relative to the prepubic blade. The area of the obturator foramen is missing in AM 6032, and poorly preserved in both pubes of AM 6150. The preserved postpubic rod is extremely thin, straight, and rod-like in AM 6150. The base of the broken rod in AM 6032 is slightly mediolaterally compressed. Although neither postpubes nor ischia are complete in AM 6150, the preserved length of the postpubic rods suggest that they extended the entire length of the ischia.

10.3 | Ischium

Both ischia are present in AM 6150; the right ischium is exposed in lateral view and missing the distal portion of the ischial blade; the right ischium is exposed in medial view, and is missing only the distal tip of the blade

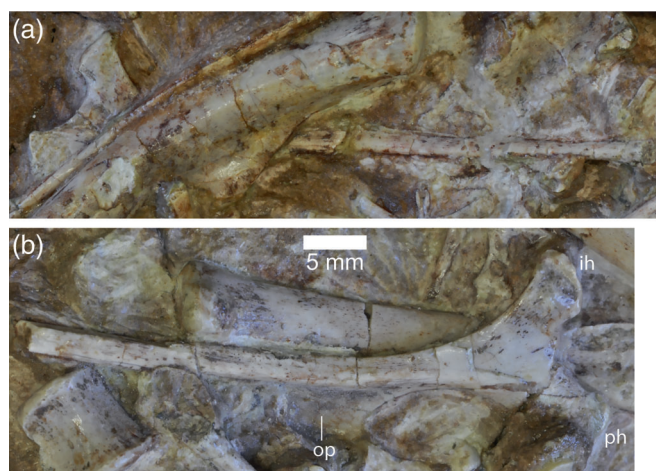


FIGURE 35 Ischia of the holotype of *Iyuku*, AM 6150. (a) Left ischium in medial view, partially obscured by femur and postpubic rod, and distal tip missing. (b) Right ischium in lateral view, distal end missing, pubic head not fully exposed. ih, iliac head; op, obturator process; ph, pubic head

although its entire obturator region is obscured beneath the right femur (Figure 35). An isolated proximal right (AM 6098) and proximal left (AM 6099) ischium are also present in the sample.

The iliac and pubic heads are well developed and separated by a broad, mediolaterally compressed, and well-embayed acetabular margin (Figure 35). Both heads are mediolaterally compressed. The iliac articular surface is nearly flat, rugose, and sub-oval in outline. The pubic head is broader than the iliac head; its articular surface is not exposed in any specimen. The large, tabular obturator process arises from the medial side of the ischial shaft, curves slightly medially towards the contralateral ischium, and is well-separated from the ischial heads (Figure 35b).

The gracile ischial shaft becomes slightly dorsoventrally compressed behind the obturator process. In contrast, most ornithopods have ischial shafts that are laterally compressed along their entire lengths (e.g., *Othnielosaurus*, *Tenontosaurus*, *Iguanodon*). However, in some taxa (e.g., *Hypsilophodon*) the medial surface of the ischial shaft twists to face dorsomedially, out of the plane of the proximal heads. In this case the ischial shaft appears dorsoventrally compressed behind the obturator process in lateral view before it broadens and flattens. Since the end of the shaft is missing in all specimens it is not known if this is the case in *Iyuku*. In AM 6150 the right ischial blade appears to be very gently curved dorsally along its length; the right blade appears to be straight although it is fractured in two places.

10.4 | Femur

Forty-seven complete to partial femora have been found at the Kirkwood Quarry representing at least 27 individuals. Complete femora range in size from 18.4 to 54.7 mm in total length ($n = 12$).

In lateral view, the largest of the femora bows slightly cranially (AM 6013, AM 6010, AM 6060, AM 6008, AM 6009), while the shafts of the smaller femora are nearly straight (e.g., AM 6163, Figure 5), suggesting that femoral curvature develops ontogenetically. In cranial view all femora appear nearly straight, although some of the larger elements bend slightly to the medial side at their distal ends (e.g., AM 6013; Figure 36).

The craniocaudally compressed femoral head is elongate, more so than in many other taxa (e.g., *Dryosaurus*, USNM 5826) (Figure 36e). A broad, shallow sulcus for the ligament of the head of the femur runs across the entire caudal surface of the femoral head, coursing ventrolaterally at approximately 45° to the horizontal in at least the larger of the juvenile sample (e.g., AM 6013, (Figure 36d,e); this area not exposed or preserved in the smallest juveniles). The proximal femur is slightly constricted between the femoral head and the trochanteric region in some juveniles (e.g., AM 6013, AM 6008, AM 6060), but not in others (e.g., AM 6010). The articular surface covers the entire head of the femur and continues laterally to the crest of the greater trochanter. The greater and lesser trochanters both rise slightly above the level of the head of the femur (Figure 36a-d). The greater trochanter is extremely craniocaudally broad, flaring dorsally and narrowing ventrally to the femoral shaft. Its lateral surface is gently convex from side to side. The lesser trochanter is very well-developed and separated along its length from the greater trochanter by a deep cleft. In proximal view, the lesser trochanter arises off the craniolateral corner at the base of the greater trochanter, and thus is not aligned with the straight crest of the greater trochanter. The lesser trochanter is flattened where it faces the greater trochanter, and bears a low crest up its cranial surface. It tapers slightly to its distal tip and its lateral surface bears a number of small dorsoventrally-oriented striations. The lesser trochanter occupies approximately 27% of the total width of the trochanteric crest (e.g., AM 6013, AM 6010, AM 6060, AM 6163) regardless of size of the individual. The trochanteric region at its widest point is approximately one and three-quarters the width of the femoral shaft below the fourth trochanter. The trochanteric region of *Iyuku* closely resembles that of other iguanodontians such as *Dryosaurus* (USNM 5826) and *Dysalotosaurus* (Janensch, 1955).



FIGURE 36 Left femur of *Iyuku*, AM 6013, in (a) lateral; (b) medial; (c) cranial; (d) caudal; (e) proximal, cranial side facing up; (f) distal, cranial side facing up, views. 4t, fourth trochanter; gt, greater trochanter; lt, lesser trochanter; s, sulcus

At the point where the trochanters meld into the shaft, the fourth trochanter arises from the caudomedial margin of the shaft as a compressed triangular structure pointing somewhat caudolaterally (Figure 36a,b). The tip of the fourth trochanter curves caudally and bears striations on its medial and lateral surfaces oriented perpendicular to its margins. On the lateral surface of the fourth trochanter is a large, oval muscle scar for the *m. caudifemoralis brevis* which extends cranially half way across the shaft and directly below the head of the femur. The distal margin of the fourth trochanter meets the shaft 48–54% of the way down the shaft in larger juveniles (femur lengths 45.1–54.7), and 51 and 53% in smaller juveniles (femur lengths 18.4 and 26.4 mm), so there does not appear to be any ontogenetic signal in the position of the fourth trochanter among this sample. Where complete, the large fourth trochanter forms a triangular fin lacking any pendant process in some specimens (e.g., AM 6150, AM 6013), and bearing a free pendant process in others (e.g., AM 6009, AM 6162, and AM 6163). The shape of the fourth trochanter does not appear to be ontogenetically controlled (e.g., AM 6150 and AM 6019 are nearly identical in size). Long, freely pendant fourth trochanters are widespread among ornithischians and early-branching ornithopods (e.g., *Scelidosaurus*, Norman, 2020; *Agilisaurus*, ZDM 6011; *Gasparinisaura*,

Coria & Salgado, 1996; *Jeholosaurus*, Han et al., 2014) but are shorter or lacking a free portion in later-branching iguanodontians (e.g., *Campitosaurus*, USNM 5818; *Iguanodon*, IRSNB 1731).

Immediately below the fourth trochanter, the femoral shaft is wider craniocaudally than it is mediolaterally, then quickly broadens mediolaterally to twice the width of the shaft as it expands to the distal condyles. There is a well-incised extensor sulcus, although there is no enclosure of the sulcus seen in any specimen (Figure 36f). The medial (tibial) condyle is very deep craniocaudally, exceeding the depth of the lateral (fibular) condyle plus the crista fibularis (“condylid”). In distal view, the cranial and medial surfaces of the medial condyle are nearly flat, while its caudal margin is convex. The articular surface of the medial condyle is gently convex front to back across its entire surface. The caudal portion of the medial condyle extends well behind the femoral shaft. The smaller lateral (fibular) condyle has a rounded cranial and lateral surface and a flatter articular surface (although it is still slightly convex). Projecting caudally from the caudomedial margin of the lateral condyle is the smaller crista fibularis. The crista is smaller and narrower than that of the medial condyle, and has a constricted base but widens slightly caudally. In distal view it is club-shaped and rounded at its caudal extremity. It does not extend as

far caudally as the tibial (lateral) condyle. In lateral view, there is a fairly well-defined sulcus extending down the lateral surface of the crista fibularis, setting it off from the rest of the lateral condyle. The distal femur of *lyuku* closely resembles that of iguanodontians such as *Tenontosaurus* (AMNH 3040) and *Dryosaurus* (Carpenter & Galton, 2018).

A deep, broad popliteal (flexor) fossa is present. Its medial margin is slightly enclosed by the caudolateral margin of the medial condyle (Figure 36f). Proximal to this the popliteal fossa is bounded by rounded epicondylar ridges that extend a short distance up the caudal surface of the femoral shaft from the medial and lateral condyles. The lateral epicondylar ridge is narrower and sharper than the medial one and also extends further proximally.

10.5 | Tibia

Tibiae are well represented in the quarry sample, including four complete, isolated right elements (AM 6012, AM 6014, AM 6089, AM 6090), and four distal tibiae (AM 6015 left, AM 6016 right, AM 6017 right, AM 6018 left) (Figure 37). Additionally, both tibiae are complete

and well preserved in AM 6150. Tibiae range in length from 59.3 (AM 6150) to 89.2 mm (AM 6089). In addition to these juvenile specimens from Kirkwood Quarry, an isolated left tibia from a larger but still immature individual (AM 6030) was collected in 1986 from a sandstone unit on the Kirkwood cliffs. This tibia is missing part of its shaft, but is estimated to be ~35 cm long, or nearly four times the length of the largest juvenile specimen from the quarry, based on measurements of the proximal and distal ends.

In lateral view the tibial shaft is perfectly straight (Figure 37a–d). In caudal view the distal half of the shaft curves medially, including a decided medial flare to the medial malleolus and the medial curve of the ascending ridge that divides the medial and lateral malleoli (e.g., AM 6012).

The mediolaterally compressed proximal tibia has a short, blunt cnemial crest that curves slightly laterally at its cranial terminus (Figure 37e). The proximal tibia is widest at the fibular (lateral) process. The fibular process extends laterally from the center of the proximal tibia and occupies approximately half or more of the proximal tibia. It extends directly laterally in some specimens (AM 6012, 6089, 6150) but angles caudolaterally in at least one individual (AM 6014). In primitive ornithopods, as well as in other



FIGURE 37 Right tibia of *Iyuku*, AM 6012 in (a) lateral; (b) medial; (c) cranial; (d) caudal; (e) proximal, cranial side facing up; (f) distal, cranial side facing up, views. afp, accessory fibular process; cc, cnemial crest; fp, fibular process

basal ornithischians such as *Scelidosaurus* (NHMUK R1111), the fibular process has a small accessory process along its craniolateral margin (e.g., *Dryosaurus*, *Hypsilophodon*). More derived ornithopods lose this extra process (e.g., *Tenontosaurus*). In *Iyuku*, this accessory fibular process is present in AM 6012 and AM 6150; its broken base can be seen in AM 6014 and AM 6089. In these specimens it is much smaller than the fibular process, and is directed craniolaterally. Caudal to the fibular process, the proximal tibia narrows to the medial condyle which exceeds the cnemial crest in mediolateral width. In at least one specimen the medial condyle also curves slightly laterally (AM 6014).

The mid shaft of the tibia narrows to approximately 31% the craniocaudal width of the proximal end. The shaft re-expands mediolaterally to the distal malleoli which are oriented nearly 90° from the long axis of the proximal end (Figure 37c,d). The malleolar width is 88% of the proximal craniocaudal width. In caudal view, the lateral malleolus is considerably longer and wider than the medial malleolus, and occupies approximately 64% the total width of the malleoli. An ascending ridge divides the medial and lateral malleolus on the caudal surface. In distal view, the surface lateral to the ascending ridge is slightly concave, while the shorter medial side is convex (Figure 37f). A blunt but extensive ridge connects the cnemial crest with the medial epicondylar ridge that rises above the medial margin of the medial malleolus. A similar ridge connects the base of the fibular processes to the lateral epicondylar ridge that rises from the lateral margin of the lateral malleolus.

In cranial view, the facet for the astragalus occupies the medial 65% of the malleoli (Figure 37c,f). The astragalar and calcaneal facets are clearly demarcated from one another on the cranial surface of the malleoli. The flat surface for articulation with the calcaneum and distal fibula is offset cranial to the fairly flat surface for the astragalar facet (Figure 37b,c,f). A slight V-shaped sulcus separates the two facets.

10.6 | Fibula

Four proximal fibulae (AM 6054 left, 6183 left, 6100 left, 6015 right) have been collected, and both complete fibulae are present in the holotype AM 6150 although only one is fully exposed (Figure 38). The fibula is 6% shorter than the tibia (AM 6150). The proximal end is mediolaterally compressed but wider at its cranial end. In proximal view the fibula is lunate; it is concave medially where it faces the tibia, and convex laterally. The proximal end quickly narrows to the shaft. In lateral view, the cranial end of the proximal fibula is more tapered than the caudal resulting in a more acute angle and a more

deeply concave cranial margin as it narrows to the shaft. The fibular shaft is mediolaterally compressed with a flattened medial surface and a rounded lateral surface. When articulated with the tibia, the caudal margin of the fibular shaft relates to the tibial epicondylar ridge that connects the fibular condyle to the lateral margin of the lateral malleolus and likely hosted the ligaments binding the fibula to the tibia. The fibular shaft narrows slightly to the distal end where it abruptly expands cranially into a small knob. The distal fibula is flat where it contacts the tibia. The distal articular surface for the calcaneum is sub-circular and convex (no calcaneum is known for *Iyuku*).

10.7 | Astragalus

Two astragali are known: AM 6015 is a left astragalus found closely associated with an articulated distal left

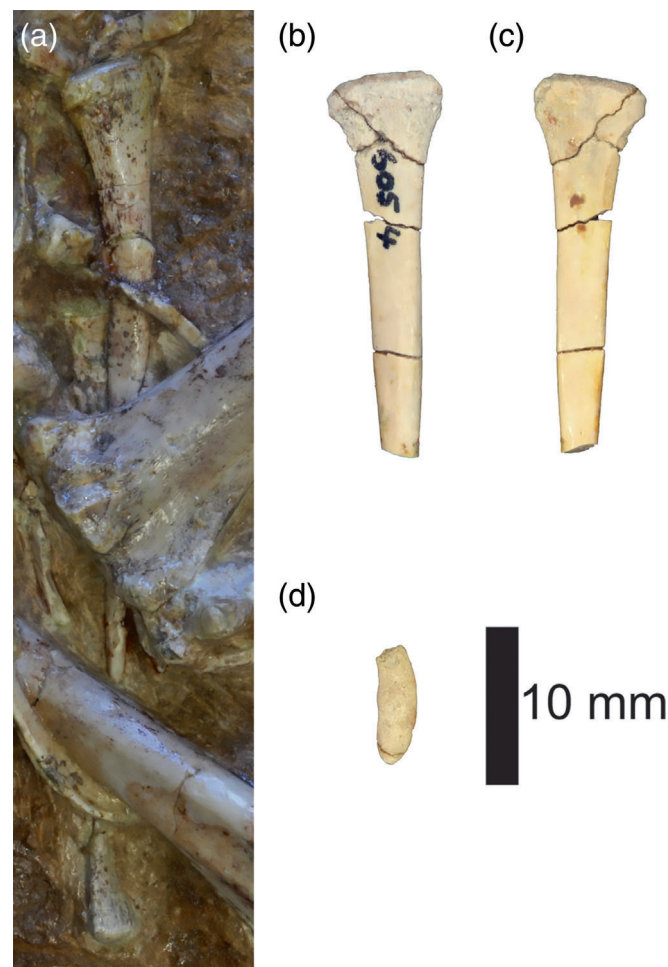


FIGURE 38 Fibulae of *Iyuku*. (a) Complete right fibula of AM 6150, partially obscured by other elements but showing the complete distal end. Proximal right fibula of AM 6054 in (a) lateral; (b) medial; (c) proximal, cranial side facing up, views

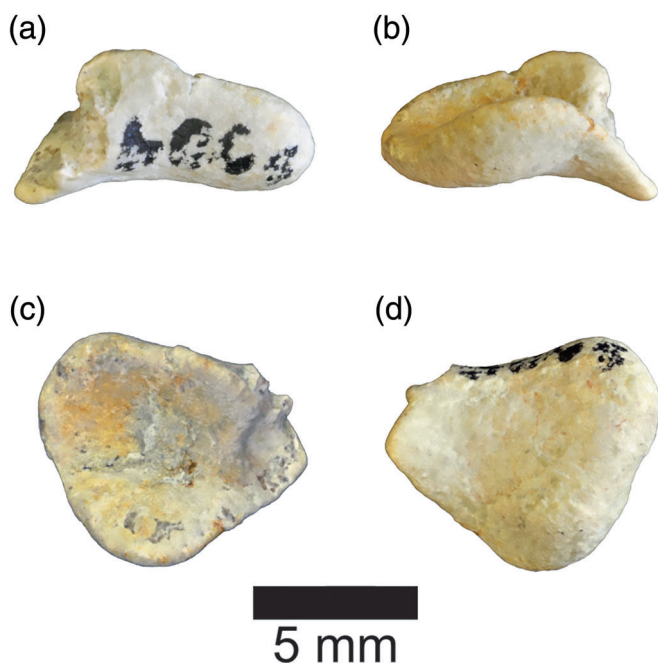


FIGURE 39 Astragalus of *Iyuku*, AM 6065 in (a) cranial; (b) caudal; (c) proximal, cranial side facing up; (e) distal, cranial side facing up, views

tibia and two metatarsals; a small part of its caudal margin is missing. AM 6065 is an isolated, complete right astragalus (Figure 39).

The astragalus caps the entire medial malleolus and part of the lateral malleolus and therefore is divided into a medial and a lateral facet, each of which is concave proximally (Figure 39c). These two facets are divided by a ridge which runs through the V-shaped sulcus that divides the medial and lateral malleoli of the tibia. The astragalus is much larger than the calcaneum and occupied 69% of the width of the distal tibia in AM 6015.

The very short cranial ascending process extends up the tibia proximal to the V-shaped sulcus (Figure 39a). The craniolateral surface of the short ascending process bears a moderately deep, well-defined facet presumably for articulation with the distal fibula. The fibula would have overlapped the lateral margin of the cranial ascending process of the astragalus as it does in many ornithischians and early-branching ornithopods (e.g., *Jeholosaurus*), but not in other ornithopods (e.g., *Tenontosaurus*). There is neither a fossa nor a foramen on the cranial aspect of the astragalus. The astragalus bears a distinct facet immediately below the facet for the fibula on the lateral margin of the ascending process, probably for articulation with the calcaneum. There is a similar short, blunt caudal ascending process that extends up to the ascending ridge on the tibia (Figure 39b). The entire medial margin of the astragalus between these ascending processes is convexly rounded and proximodistally thick. The lateral portion of the astragalus is much

smaller and less robust than the medial portion, and compresses laterally to a thin edge (much thinner than the medial margin). No calcaneum or distal tarsals have been recovered or identified.

10.8 | Pes

Complete metatarsals (MT) III and IV are preserved with AM 6150 along with three other unidentified partial metatarsals. Two partial metatarsals (distal MT I and proximal MT IV) were found with the distal tibia and astragalus of AM 6015. Two complete, isolated left MT I were collected from the quarry (AM 6121, 6174) (Figure 40).

In MT I the proximal end is mediolaterally compressed and dorsoplantarly expanded, slightly convex laterally and concave medially where it attaches to MT II. In lateral view the proximal end is convex. The shaft is straight and mediolaterally compressed to the same degree as the proximal end. In lateral view the shaft reduces in height distally to approximately half the height of the proximal end before re-expanding dorsoplantarly, as well and mediolaterally, to the distal condyles. MT I is flattened along its lateral side to fit snuggly against MT II. The distal end is also somewhat dorsoplantarly expanded and mediolaterally compressed. The condyles lack a ginglymus. The dorsal aspect of the condyles is rounded and each condyle expands plantarly into flexor processes that are separated by a sulcus on the ventral aspect. A very shallow and poorly defined ligament depression indents the medial and lateral side of the condyles. In dorsal view the condylar surface is angled slightly medially, away from the rest of the pes.

The left MT III is exposed in ventral view in AM 6150 and partially obscured by the right ischium (Figure 40g). The shaft is straight and expands slightly but equally to the proximal and distal ends of the element. The distal condyles are divided by a ginglymus and are asymmetrical with the lateral condyle being slightly wider than the medial condyle.

The right MT IV is exposed in AM 6150 (Figure 40h). It is 47% the length of the femur, and 40% the length of the tibia. The distal articular end is not exposed. The shaft is straight and the proximal end appears to be triangular and expands dorsally.

AM 6033 is an isolated ungual of a subadult individual (Figure 40i–k). The ungual is long and subrounded at its tip and dorsoventrally compressed. The proximal articular surface is asymmetrical and divided into two facets, one being wider, taller, and slightly more proximally positioned than the other. The ungual curves slightly towards the smaller side. This indicates that this is the ungual for either the second or fourth digit. There is a

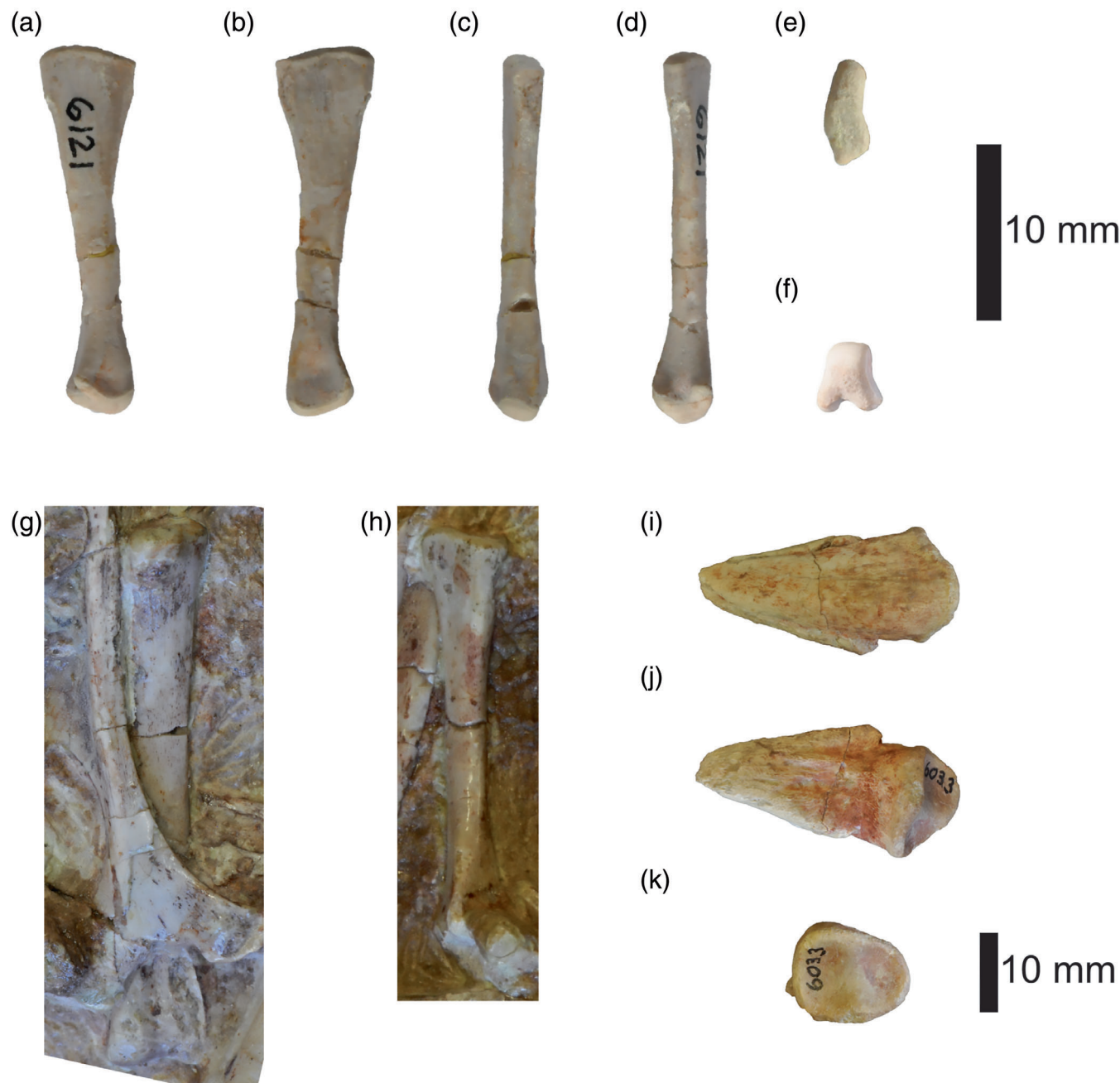


FIGURE 40 Pedal elements of *Iyuku*. Left metatarsal I of AM 6121 in: (a) medial; (b) lateral; (c) dorsal; (d) ventral; (e) proximal, plantar side up; (f) distal views. (g) left metatarsal III of AM 6150 in ventral view. (h) right metatarsal IV ventrolateral view. Pedal ungual of AM 6033 in (i) dorsal; (j) ventral; (k) proximal, dorsal side up, views

slight ridge down the center of the ungual on the ventral surface. Well-developed sulci run down the distal three-quarters of the plantaromedial and platarolateral surfaces of the ungual.

The extremely straight shafts of MT I, II, and IV are unlike the pes of many ornithopods where curvature of MT II through IV is the norm (e.g., *Tenontosaurus*, Forster, 1990; *Iguanodon*, Norman, 1980). Some early-branching ornithischians tend to have straight or nearly straight metatarsals (e.g., *Othnielosaurus* [*Nanosaurus*],

BYU 163; *Hexinlusaurus*, ZDM 6001). However, it is also possible that curvature is ontogenetically driven and the straight nature of the metatarsals in *Iyuku* are due to their young status.

11 | DISCUSSION

The bone histology of the young individuals of *Iyuku* reveals multiple faint rest lines, indicating they may have

been subjected to periodic stress severe enough to briefly arrest their growth early in ontogeny, and that may have ultimately resulted in their deaths. These growth interruptions occur in multiple individuals, suggesting that the stressor was external and may have resulted from an environmental factor.

The bonebed horizon heralds a shift in sedimentology and possibly climate up section, and is indicative of a more arid and seasonal environment. Its occurrence within the Bss (slickenside) horizon of a well-developed Vertisol indicates not only a period of relative stasis in sedimentation, but periods of intense aridity. We hypothesize that the external stress placed on the *Iyuku* juveniles may have involved these drier, more seasonal, and likely hotter conditions. The stress that arrested the growth of the juveniles may have been dry and drought-like conditions, repeated periods of extreme heat, or a combination of both. While this climatic shift may be coincidental with the bonebed accumulation, it also offers a possible explanation for the stress and high mortality experienced by the young individuals of *Iyuku*. Therefore climate change may have played an important role in the genesis of this fossil accumulation.

Numerous morphological features of *Iyuku* attest to its phylogenetic position within Iguanodontia. *Iyuku* occurs temporally between the Late Jurassic *Dysalotosaurus* in Tanzania and the Late Cretaceous *Kangnasaurus* in South Africa. This sparse record of iguanodontians specifically and ornithopods generally may be due to a lack of recognized fossil-bearing sediments spanning the Cretaceous, and highlights the likelihood that iguanodontians were present in southern Africa throughout the Cretaceous.

AUTHOR CONTRIBUTIONS

Catherine A. Forster: Conceptualization (equal); formal analysis (lead); funding acquisition (equal); investigation (equal); methodology (supporting); project administration (equal); supervision (lead); visualization (supporting); writing – original draft (lead); writing – review and editing (lead). **William J. de Klerk:** Conceptualization (equal); funding acquisition (equal); investigation (equal); project administration (equal); writing – original draft (supporting). **Karen E. Poole:** Formal analysis (equal); visualization (lead); writing – original draft (supporting). **Anusuya Chinsamy-Turan:** Formal analysis (lead); investigation (equal); methodology (equal); visualization (supporting); writing – original draft (supporting). **Eric M. Roberts:** Formal analysis (supporting); investigation (lead); visualization (supporting); writing – original draft (supporting). **Callum F. Ross:** Funding acquisition (equal); investigation (equal); project administration (equal); writing – original draft (supporting).

ACKNOWLEDGMENTS

We thank the Albany Museum for logistic and material support for field and laboratory work. The collection of these specimens represents 3 years of quarrying efforts, and we gratefully acknowledge the hard work and companionship of the 1995, 1997, and 1999 field crews: Brian Curtice, Linda Curtice, Kristina Curry Rogers, Andrew de Klerk, Sue Frost, Priscilla Hall, Lea Ann Jolly, Patrick O'Connor, Donna Rowsell, Nancy Stevens, and Blythe Williams. We particularly thank Brian Curtice for recognizing the articulated nature of AM 6150 and carefully collecting the specimen in a field jacket. Jean-Pierre Cavigelli and Virginia Heisey expertly prepared some of the specimens described here. Two anonymous reviewers provided excellent suggestions for refining this manuscript. Grant sponsors: The Dinosaur Society, The Jurassic Foundation, and The George Washington University. Our co-author, Billy de Klerk, passed away shortly before the publication of this manuscript. We mourn the loss of our friend and colleague—the epitome of a true gentleman and scholar.

ORCID

Catherine A. Forster  <https://orcid.org/0000-0002-3032-2399>

Karen E. Poole  <https://orcid.org/0000-0001-9781-4972>
Anusuya Chinsamy-Turan  <https://orcid.org/0000-0002-9786-5080>

REFERENCES

- Andrzejewski, K. A., Winkler, D. A., & Jacobs, L. L. (2019). A new basal ornithopod (Dinosauria: Ornithischia) from the Early Cretaceous of Texas. *PLoS One*, 14(3), e0207935.
- Atherstone, W. G. (1857). Geology of Uitenhage. *Eastern Province Monthly Magazine*, 1, 518–532.
- Barrett, P., & Han, F. L. (2009). Cranial anatomy of *Jeholosaurus shangyuensis* (Dinosauria: Ornithischia) from the Early Cretaceous of China. *Zootaxa*, 2072, 31–55.
- Baur, G. (1891). Remarks on the reptiles generally called Dinosauria. *The American Naturalist*, 25, 434–454.
- Brochu, C. A. (1996). Closure of neurocentral sutures during crocodilian ontogeny: Implications for maturity assessment in fossils archosaurs. *Journal of Vertebrate Paleontology*, 16, 49–62.
- Broom, R. (1904). On the occurrence of an opisthocoelian dinosaur (*Algosaurus bauri*) in the cretaceous beds of South Africa. *Geological Magazine*, 1, 445–477.
- Carpenter, K. (1994). Baby *Dryosaurus* from the upper Jurassic Morrison formation of Utah and Colorado. In K. Carpenter, D. Chure, & J. Horner (Eds.), *Dinosaur Eggs and Babies* (pp. 288–297). Cambridge University Press.
- Carpenter, K., & Galton, P. M. (2018). Photo documentation of bipedal ornithischian dinosaurs from the Upper Jurassic Morrison Formation, USA. *Geology of the Intermountain West*, 5, 167–207.
- Cerda, I. A., & Chinsamy, A. (2012). Biological implications of the bone microstructure of the late cretaceous ornithopod dinosaur

- Gasparinisaura cincosalensis*. *Journal of Vertebrate Paleontology*, 32, 355–368.
- Chinsamy-Turan, A. (2005). *The microstructure of dinosaur bone: Deciphering biology with fine-scale techniques* (1st ed.). Johns Hopkins University Press.
- Chinsamy, A., Thomas, D. B., Tumarkin-Deratzian, A., & Fiorillo, A. R. (2012). Hadrosaurs were perennial polar residents. *The Anatomical Record*, 295(4), 610–614.
- Choiniere, J., Forster, C. A., & de Klerk, W. J. (2012). New information on *Nqwebasaurus thwazi*, a coelurosaurian theropod from the Early Cretaceous Kirkwood Formation in South Africa. *Journal of African Earth Sciences*, 71–72, 1–17.
- Cooper, M. R. (1985). A revision of the ornithischian dinosaur *Kangnasaurus coetzeei* Haughton, with a classification of the Ornithischia. *Annals of the South African Museum*, 95, 281–317.
- Coria, R. A., & Salgado, L. (1996). A basal iguanodontian (Ornithischia: Ornithopoda) from the Late Cretaceous of South America. *Journal of Vertebrate Paleontology*, 16(3), 445–457.
- Coria, R. A., & Calvo, J. O. (2002). A new iguanodontian ornithopod from Neuquen Basin, Patagonia, Argentina. *Journal of Vertebrate Paleontology*, 22(3), 503–509.
- De Klerk, W. J., Forster, C. A., Ross, C. F., Sampson, S. D., & Chinsamy, A. (1998). A review of recent dinosaur and other vertebrate discoveries in the Early Cretaceous Kirkwood Formation in the Algoa Basin, Eastern Cape, South Africa. *Journal of African Earth Sciences*, 27(1), 55.
- De Klerk, W. J., Forster, C. A., Sampson, S. D., Chinsamy, A., & Ross, C. F. (2000). A new coelurosaurian dinosaur from the Early Cretaceous of South Africa. *Journal of Vertebrate Paleontology*, 20, 324–332.
- De Wit, M. C. J., Ward, J. D., & Spaggiari, R. (1992). A reappraisal of the Kangnas dinosaur site, Bushmanland, South Africa. *South African Journal of Science*, 88, 504–507.
- Dilkes, D. (2001). An ontogenetic perspective on locomotion in the Late Cretaceous dinosaur *Maiasaura peeblesorum* (Ornithischia: Hadrosauridae). *Canadian Journal of Earth Sciences*, 38(8), 1205–1227.
- Dodson, P. (1980). Comparative osteology of the American ornithopods *Camptosaurus* and *Tenontosaurus*. *Memoires de la Societe Geologiques de France*, 139, 81–85.
- Forster, C. A. (1990). The postcranial skeleton of the ornithopod dinosaur *Tenontosaurus tilletti*. *Journal of Vertebrate Paleontology*, 10, 273–294.
- Forster, C. A., Frost, S., & Ross, C. F. (1995). New dinosaur material and paleoenvironment of the Early Cretaceous Kirkwood Formation, Algoa Basin, South Africa. *Journal of Vertebrate Paleontology*, 15, 29.
- Forster, C. A., & de Klerk, W. J. (2008). Preliminary report on a new basal iguanodontian dinosaur from the Early Cretaceous Kirkwood Formation, South Africa. In 15th Biennial Conference of the Palaeontological Society of Southern Africa, Matjiesfontein, 12–16 September 2008, Abstract volume: 98.
- Forster, C. A., Farke, A. A., McCartney, J. A., de Klerk, W. J., & Ross, C. F. (2009). A “basal” Tetanuran from the Lower Cretaceous Kirkwood Formation of South Africa. *Journal of Vertebrate Paleontology*, 29, 56–64.
- Frost, S. (1996). Early Cretaceous alluvial palaeosols (Kirkwood Formation, Algoa Basin, South Africa) and their palaeoenvironmental and palaeoclimatological significance [Unpublished M. Sc. Thesis]. Rhodes University, Grahamstown, South Africa, pp. 1–177.
- Galton, P. M. (1974). The ornithischian dinosaur *Hypsilophodon* from the wealdon of the isle of wight. *Bulletin of the British Museum (Natural History) Geology*, 25, 1–152.
- Galton, P. M. (1983). The cranial anatomy of *Dryosaurus*, a hypsilophodontid dinosaur from the Upper Jurassic of North America and East Africa, with a review of hypsilophodontids from the Upper Jurassic of North America. *Geologica et Paleontologica*, 17, 207–243.
- Galton, P. M., & Coombs, W. P., Jr. (1981). *Paranthodon africanus* (Broom) a segosaurian dinosaur from the Lower Cretaceous of South Africa. *Géobios*, 14, 299–309.
- Han, F. L., Barrett, P. M., Butler, R. J., & Xu, X. (2014). Postcranial anatomy of *Jeholosaurus shangyuanensis* (Dinosauria, Ornithischia) from the Lower Cretaceous Yixian Formation of China. *Journal of Vertebrate Paleontology*, 32(6), 1370–1395.
- Haughton, S. H. (1915). On some dinosaur remains from Bushmanland. *Transactions of the Royal Society of South Africa*, 5, 259–264.
- Head, J. J. (1998). A new species of basal hadrosaurid (Dinosauria, Ornithischia) from the Cenomanian of Texas. *Journal of Vertebrate Paleontology*, 18(4), 718–738.
- Horner, J. R. (1994). Comparative taphonomy of some dinosaur and extant bird colonial nesting grounds. In K. Carpenter, K. F. Hirsch, & J. R. Horner (Eds.), *Dinosaur Eggs and Babies* (pp. 116–123). Cambridge University Press.
- Horner, J. R., & Currie, P. J. (1994). Embryonic and neonatal morphology and ontogeny of a new species of *Hypacrosaurus* (Ornithischia, Lambeosauridae) from Montana and Alberta. In K. Carpenter, K. F. Hirsch, & J. R. Horner (Eds.), *Dinosaur Eggs and Babies* (pp. 312–336). Cambridge University Press.
- Horner, J. R., de Ricqlés, A., & Padian, K. (2000). The bone histology of the hadrosaurid dinosaur *Maiasaura peeblesorum*: Growth dynamics and physiology based on an ontogenetic series of skeletal elements. *Journal of Vertebrate Paleontology*, 20, 109–123.
- Horner, J. R., Padian, K., & de Ricqlés, A. (2001). Comparative osteohistology of some embryonic and perinatal archosaurs: Developmental and behavioral implications for dinosaurs. *Paleobiology*, 27, 39–58.
- Hübner, T. R., & Rauhut, O. (2010). A juvenile skull of *Dysalotosaurus lettowvorbecki* (Ornithischia: Iguanodontia), and implications for cranial ontogeny, phylogeny, and taxonomy in ornithopod dinosaurs. *Zoological Journal of the Linnean Society*, 160, 366–396.
- Hübner, T. R. (2012). Bone histology in *Dysalotosaurus lettowvorbecki* (Ornithischia: Iguanodontia): Variation, growth, and implications. *Plos One, January*, 7, e29958.
- Janensch, W. (1955). Der Ornithopode *Dysaltosaurus* der Tendaguru-schichten. *Palaeontographica*, 3(7), 97–103.
- Knoll, F., Padian, K., & de Ricqlés, A. (2010). Ontogenetic change and adult body size of the early ornithischian dinosaur *Lesothosaurus diagnosticus*: Implications for basal ornithischian taxonomy. *Gondwana Research*, 17, 171–179.
- Mack, G. H., James, W. C., & Monger, H. C. (1993). Classification of paleosols. *Geological Society of America Bulletin*, 105, 129–136.
- Makaske, B. (2001). Anastomosing rivers: A review of their classification, origin and sedimentary products. *Earth-Science Reviews*, 53, 149–196.

- Makovicky, P. J., Kilbourne, B. M., Sadleir, R. W., & Norell, M. A. (2014). A new basal ornithopod (Dinosauria, Ornithischia) from the Late Cretaceous of Mongolia. *Journal of Vertebrate Paleontology*, 31, 626–640.
- Marsh, O. C. (1881). Classification of the Dinosauria. *American Journal of Science*, 23, 81–86.
- Maryanska, T., & Osmólska, H. (1974). Pachycephalosauria, a new suborder of ornithischian dinosaurs. *Paleontologia Polonica*, 30, 45–122.
- McDonald, A. T., Maidment, S. C. R., Barrett, P. M., You, H., & Dodson, P. (2014). Osteology of the basal hadrosauroid *Equijubus normani* (Dinosauria, Ornithopoda) from the Early Cretaceous of China. In D. A. Eberth & D. C. Evans (Eds.), *Hadrosaurs* (pp. 44–72). Indiana University Press.
- McLachlan, I. R., & McMillan, I. K. (1976). Review and stratigraphic significance of Southern Cape Mesozoic palaeontology. *Transaction of the Geological Society of South Africa*, 79, 197–212.
- McMillan, I. K. (2003). The foraminifera of the Late Valanginian to Hauterivian (Early Cretaceous) Sundays River Formation of the Algoa Basin, Eastern Cape Province, South Africa. *Annals of the South African Museum*, 106, 1–274.
- Miall, A. D. (1985). Architectural-element analysis: A new method of facies analysis applied to fluvial deposits. *Earth Sciences Reviews*, 22, 261–308.
- Muir, R. A., Bordy, E. M., Reddering, J. S. V., & Viljoen, J. H. A. (2017a). Lithostratigraphy of the Kirkwood Formation (Uitenhage group), including the Bethelsdorp, Colchester and Swartkops members, South Africa. *South African Journal of Geology*, 120(2), 281–293.
- Muir, R. A., Bordy, E. M., Reddering, J. S. V., & Viljoen, J. H. A. (2017b). Lithostratigraphy of the Enon Formation (Uitenhage group), South Africa. *South African Journal of Geology*, 120(2), 271–280.
- Muir, R. A., Bordy, E. M., Mundil, R., & Frei, D. (2020). Recalibrating the breakup history of SW Gondwana: U–Pb radioisotopic age constraints from the Southern Cape of South Africa. *Gondwana Research*, 84, 177–193.
- Nadon, G. (1994). The genesis and recognition of anastomosed fluvial deposits: Data from the St. Mary River Formation, southwestern Alberta, Canada. *Journal of Sedimentary Research B*, 64, 451–463.
- Norman, D. B. (1980). On the ornithischian dinosaur *Iguanodon bernissartensis* from the Lower Cretaceous of Bernissart (Belgium). *Institut Royal des Sciences Naturelles de Belgique Mémoire*, 178, 1–104.
- Norman, D. B. (2002). On Asian ornithopods (Dinosauria: Ornithischia). 4. *Probactrosaurus* Rozdestvensky, 1966. *Zoological Journal of the Linnean Society*, 136, 113–144.
- Norman, D. B. (2004). Basal iguanodontia. In D. B. Weishampel, P. Dodson, & M. Osmolska (Eds.), *The Dinosauria* (pp. 413–437). University of California Press.
- Norman, D. B. (2020). *Scelidosaurus harrisonii* from the Early Jurassic of Dorset, England: Postcranial skeleton. *Zoological Journal of the Linnean Society*, 189, 47–157.
- Owen, R. (1842). Report on British fossil reptiles. Part II. In 11th Meeting of the Report of the British Association for the Advancement of Science 11, pp. 60–204.
- Poole, K. E. (2015). Phylogeny and biogeography of Iguanodontian dinosaurs, with implications from ontogeny and an examination of the function of the fused carpal-metacarpal complex [PhD Dissertation]. The George Washington University, pp. 1–207.
- Raven, T. J., & Maidment, S. C. R. (2018). The systematic position of the enigmatic thyreophoran dinosaur *Paranthodon africanus*, and the use of basal exemplifiers in phylogenetic analysis. *PeerJ*, 6, e4529.
- Reddering, J. S. V. (2012). *Kirkwood Formation (Uitengage Group), including the Swartkops and Colchester members*. South African Committee for Stratigraphy, Council for Geoscience, Catalogue of South African Lithostratigraphic Units.
- Retallack, G. J. (1990). *Soils of the past* (p. 10520). Springer.
- Rich, T. H. V., Molnar, R. E., & Rich, P. V. (1983). Fossil vertebrates from the Late Jurassic or Early Cretaceous Kirkwood Formation, Algoa Basin, Southern Africa. *Transactions of the Geological Society of South Africa*, 86, 281–291.
- Rigassi, D., & Dixon, G. E. (1972). Cretaceous of the Cape Province, Republic of South Africa. In Proceedings of the Conference on African Geology, Dec. 1970, Ibadan University, Nigeria, pp. 513–527.
- Rogers, A. W. (1915). The occurrence of dinosaurs in Bushmanland. *Transactions of the Royal Society of South Africa*, 5, 265–272.
- Ross, C. F., Sues, H.-D., & de Klerk, W. J. (1999). Lepidosaurian remains from the Lower Cretaceous Kirkwood Formation of South Africa. *Journal of Vertebrate Paleontology*, 19, 21–27.
- Sampson, S. D., Ryan, M. J., & Tanke, D. H. (1997). Craniofacial ontogeny in centrosaurine dinosaurs (Ornithischia: Ceratopsidae): Taxonomic and behavioral implications. *Zoological Journal of the Linnean Society*, 121, 293–337.
- Seely, H. G. (1888). The classification of the Dinosauria. Report of the British Association for the Advancement of Science 1887, pp. 698–699.
- Shone, R. W. (1976). The sedimentology of the Mesozoic Algoa Basin [M.Sc. Dissertation]. University of Port Elizabeth, 48 pp.
- Shone, R. W. (1978). A case for lateral gradation between the Kirkwood and Sundays River formations, Algoa Basin. *Transaction of the Geological Society of South Africa*, 81, 319–326.
- Shone, R. W. (2006). Onshore post-Karoo Mesozoic deposits. In M. R. Johnson, C. R. Anhaeusser, & R. J. Thomas (Eds.), *The geology of South Africa* (pp. 541–571). Council for Geoscience and Geological Society of South Africa.
- Smith, D. G. (1987). Meandering river point bar lithofacies models: Modern and ancient examples compared. In F. G. Ethridge, R. M. Flores, & M. D. Harvey (Eds.), *Recent developments in fluvial sedimentology* (Vol. 39, pp. 83–91). Society of Economic Paleontologists and Mineralogists Special Publication.
- Smith, R. M. H. (1986). Sedimentation and palaeoenvironments of Late Cretaceous crater-lake deposits in Bushmanland, South Africa. *Sedimentology*, 33, 369–386.
- Tankard, A. J., Jackson, M. P. A., Eriksson, K. A., Hobday, D. K., Hunter, D. R., & Mitwe, W. E. L. (1982). *Crustal evolution of southern Africa: 3.8 billion years of earth history* (p. 532). Springer.
- Taquet, P. (1976). *Geologie et paleontologie du gisement de Gadoufaoua (Aptien du Niger)*, Cahier des Paleontologie (pp. 1–191). C.N.R.S. Paris.

- Thomas, D. A. (2015). The cranial anatomy of *Tenontosaurus tilletti* Ostrom, 1970 (Dinosauria, Ornithopoda). *Paleontologia Electronica*, 18.2.37A, 1–99.
- Toerien, D. K., & Hill, R. S. (1989). The geology of the Port Elizabeth area. Explanation, geological sheet 3324 Port Elizabeth, scale 1:250 000, Geological Survey, Pretoria, South Africa, 35 pp.
- Törnqvist, T. E. (1993). Holocene alternation of meandering and anastomosing fluvial systems in the Rhine–Meuse delta (central Netherlands) controlled by sea-level rise and sub-soil erodability. *Journal of Sedimentary Petrology*, 63, 683–693.
- Tumarkin-Deratzian, A. R., Vann, D. R., & Dodson, P. (2006). Bone surface texture as an ontogenetic indicator in long bones of the Canada goose *Branta canadensis* (Anseriformes: Anatidae). *Zoological Journal of the Linnean Society*, 148, 138–168.
- Tumarkin-Deratzian, A. R. (2009). Evaluation of long bone surface textures as ontogenetic indicators in centrosaurine ceratopsids. *The Anatomical Record*, 292, 1485–1500.
- Weishampel, D. B., Jianu, C.-M., Csiki, Z., & Norman, D. B. (2003). Osteology and phylogeny of *Zalmoxes* (N. G.), an unusual euornithopod dinosaur from the latest Cretaceous of Romania. *Journal of Systematic Palaeontology*, 1, 65–123.
- Winter, H. D. L. R. (1973). Geology of the Algoa Basin, South Africa. In G. Blant (Ed.), *Sedimentary basins of South African coast, 2nd part (South and East Coast)* (pp. 17–48). Association of African Geological Surveys.

How to cite this article: Forster, C. A., de Klerk, W. J., Poole, K. E., Chinsamy-Turan, A., Roberts, E. M., & Ross, C. F. (2022). *Iyuku raathi*, a new iguanodontian dinosaur from the Early Cretaceous Kirkwood Formation, South Africa. *The Anatomical Record*, 1–42. <https://doi.org/10.1002/ar.25038>